Supplementary Information for

Highly Sensitive Nanochannel Device for the Detection of SUMO1 Peptides

Yue Qin,[#a, b] Xiaoyu Zhang,[#b] Yanling Song,[a] Bowen Zhong,[b] Lu Liu[b], Dongdong Wang,[b] Yahui Zhang,[b] Wenqi Lu,[b] Xinjia Zhao,[b] Zhiqi Jia,[a] Minmin Li,[b] Lihua Zhang*[b] and Guangyan Qing*[b, c]

[a]College of Pharmaceutical and Biological Engineering, Shenyang University of Chemical Technology, No. 11 Street, Economic and Technological Development Zone, Shenyang 110142, P. R. China

[b]CAS Key Laboratory of Separation Science for Analytical Chemistry, Dalian Institute of Chemical Physics, Chinese Academy of Sciences, 457 Zhongshan Road, Dalian 116023, P. R. China.

[c]College of Chemistry and Chemical Engineering, Wuhan Textile University, 1 Sunshine Road, Wuhan 430200, P. R. China.

Table of Contents

Section 1. Materials and Instruments

2-mercaptoethanol was purchased from Aladdin Co., Ltd. (China). Polyethylene terephthalate (PET) films with 12 μm in thickness and 30 mm in diameter were irradiated at the linear accelerator UNILAC (GSI, Darmstadt) with swift heavy ions having an energy of 11.4 MeV per nucleon with 10^7 ions/cm^2 ion tracks in the center. Dithiothreitol (DTT) was purchased from Beijing InnoChem Co., Ltd. (China). A phage display peptide library and Escherichia coli ER2738 host cells were purchased from (New England Bio-labs, MA, USA). Standard peptides were purchased from Synpeptide Co., Ltd (Shanghai, China). SENP1 was purchased from LifeSensors (Malven, PA, USA). Potassium ferricyanide and potassium ferrocyanide were purchased from Macklin Biochemical Co., Ltd. (Shanghai, China). Tris (hydroxymethyl) aminomethane (≥ 98%) was purchased from Solarbio Technologier Co., Ltd. α-Al_2O_3 (0.3 and 0.05 μm) were purchased from Chenhua Instrument Co., Ltd. (Shanghai China). 1-ethyl-3-(3-dimethylaminopropyl) carbodiimide hydrochloride (EDC), N-hydroxy succinimide (NHS) were purchased from Aladdin Co., Ltd. (China). Other solvents and reagents were purchased from Sinopharm Chemical Reagent Co., Ltd. (China). RQ5MTAP QC chips were purchased from Shenzhen Renlu Technology Co., Ltd. (China). Water used in this study was purified by Milli-Q system (18.2 MΩ·cm).

All nuclear magnetic resonance (NMR) spectra were recorded on Bruker Avance III 400M NMR spectrometer (Bruker Corp., Germany). Ultraviolet visible (UV–Vis) spectra were obtained through a PerkinElmer LAMBDA 365 UV–Vis Spectrophotometer. X-ray photoelectron spectroscopy (XPS) data were obtained with an ESCALAB250xi (Thermo Fisher Scientific, US). All current–voltage (I–V) curves were measured by a Keithley 6487 picoammeter (Tektronix Inc., USA). Electrochemical impedance experiments (EIS), Faraday current and Cyclic voltammetry (CV) were carried out on a CHI 760E electrochemical workstation (CH Instruments, Shanghai, China). Surface contact angle (CA) data were obtained from KRUSS DSA 100 (KRÜSS GmbH, Germany). Infrared (IR) spectra were recorded on a Bruker Vertex 80v Fourier transform infrared (FT-IR) spectrometer in combination with a bio-attenuated total reflection (ATR) accessory. Field emission scanning electron microscopy (FESEM) images of PET nanochannels with base side, tip side and crosse section were obtained

by JSM 7800F (JEOL Ltd, Japan) after platinum spray treatment. Dynamic adsorption experiments were performed in a quartz crystal microbalance with dissipation monitoring (QCM-D, Q-Sense E4 system, Biolin Scientific Corp., Sweden). Surface potential was measured with Bruker Dimension Icon atomic force microscope (AFM) in the mode of Kelvin Probe Force Microscope (KPFM). Metallization of PET films was done on the LN-FS1024 coater (Shenyang Lining Vacuum Technology Research Institute, China). Cell imaging data were obtained on the FV1000MPE two-photon confocal microscope system (Olympus Japan Co., Ltd.).

Section 2. Experiment methods

Section 2.1 Phage display biopanning for the SUMO1-binding CPs

To identify SUMO1-binding CPs, we performed phage display screening including one round of reverse biopanning against BSA followed by four rounds affinity biopanning against DG12, as described previously.[1, 2] After completing all biopanning procedures, phages were randomly selected for DNA sequencing. Phage DNA was extracted by using M13 single-stranded DNA extraction kit (BioTeke, China) and DNA sequencing was entrusted to Shanghai Sangon Biotech Corporation (Shanghai, China). Enzyme-linked immunosorbent assay (ELISA) was used to evaluate the affinity of phage clones toward DG12. The ELISA plate coated with DG12 was gently shaken overnight at 4°C. Then, 0.5% BSA blocking buffer was added and incubated for 1 h. After washing with 0.05% TBST, monoclonal phages were added to each well and incubated at room temperature for 1 h. Subsequently, the plate was incubated with HRP-conjugated anti-M13 monoclonal antibody (1:5000) for 1 h, followed by 0.05% TBST. Finally, according to the EL-ABTS (C510031, Sangon Biotech, China) manufacturer's instructions, the reaction buffer and the stop buffer were added. The absorbance of 405 nm was measured by an FC microplate reader (Thermo Fisher Scientific, US).

Section 2.2 Fabrication of PET conical nanochannels

The conical nanochannels were fabricated by the ion track etching technique developed by Apel *et al.* and some improved steps.[3-6] First, two sides of the multiple ion-irradiated PET film with 1×10^7 ion tracks per square centimeter were treated with UV light for 30 min. The

PET film was then mounted on a stainless steel holder for two special Teflon modules (with a central hole for 5 mm diameter for etching), in which the film acted as an isolation valve. The cavity of one Teflon module is filled with etching solution (9 M NaOH) and the other with stop solution (1 M HCOOH + 1 M KCl), etching was carried out at 45°C. Meanwhile, a potential of 1 V was applied for monitoring the etching process, transmembrane ionic current could be observed when nanochannels opened. The etching solution was replaced by a stop solution when the ionic current reached a certain desired value and then washed with ultrapure water to remove residual salts, finally, the conical nanochannels of PET film was removed and immersed in water.

Section 2.3 Preparation of CP-1-modified nanochannels

The metal layer was deposited controllably by a coater, a 40 nm thick layer of nickel and gold was sputtered onto the tip side of PET film at a deposition rate of 0.02 $nm \cdot s^{-1}$. This process can be finely tuned by deposition rate and time to obtain metalized solid state nanochannels. The metalized films were rinsed with ultrapure water and ethanol respectively. PET film was sandwiched in a homemade electrochemical cell and 2 mL of Tris-HCl buffer solution (TBS, 5 mM, pH 8.0) containing 0.25 mM CP-1 was added and left for 12 h, followed by treatment with TBS containing the same concentration of 2-mercaptoethanol for 4 h, which was used to occupy the excess gold atomic sites.

The modified PET film was continued to be mounted in the electrochemical cell, rinsed with TBS, a voltage of –2 V to +2 V was applied with a step time of 1s and a step voltage of 0.2 V. The current across membrane was measured with a pair of platinum wire electrodes, and the transmembrane ionic current was measured by a Keithley 6487 picoammeter (Tektronix Inc., USA); as for Faraday current, increments of 4 mV, amplitude of 50 mV and frequency of 10 Hz, the metal-modified PET film was used as the working electrode, with the platinum wire electrode and Ag/AgCl saturated electrode from a three-electrodes system. The current signals were recorded by CHI 630D electrochemical workstation (Shanghai, China). TBS was used to equip the guest solutions with different concentrations and the current was measured every 5 min. Average currents were obtained by repeating the measurements three times independently.

Section 2.4 Surface CA measurements

Three PET films were etched for the same time and process as used to simulate PET nanochannels, one of them was immersed overnight in Milli-Q water, the others were metal deposited, one of the films was selected to be modified with CP-1 and finally the three films were washed with ultrapure water and blown dry with N_2. CA measurements were carried out at ambient temperature with approximately 10 μL of water drops onto the sample surface for each measurement, and average contact angles were obtained at three different locations on the same membrane.

Section 2.5 Trypsin digestion of bovine serum albumin (BSA)

The experiment was carried out in accordance with a previously reported.[7] One milligram of BSA was dissolved in 100 μL of 6 M urea in 50 mM NH_4HCO_3 solution. The protein solution was then subjected to a treatment with 20 μL of 200 mM dithiothreitol (DTT) for 45 minutes at a temperature of 56°C. Subsequently, 80 μL of 200 mM iodoacetamide was added to the mixture and incubated in the dark for 30 minutes at room temperature. The mixture was then diluted to 1 mL with 50 mM NH_4HCO_3 solution and digested with trypsin at an enzyme to protein mass ratio of 1:40 and incubated overnight at 37°C. Finally, the resulting tryptic mixture was loaded onto a homemade C18 tip and eluted with a solution of 75% acetonitrile and 0.1% formic acid.

Section 2.6 EIS measurements

EIS measurements were carried out on a CHI 760E electrochemical workstation. The gold electrode (3 mm diameter) was first immersed in a mixture of H_2O: $NH_3 \cdot H_2O$: H_2O_2 (5:1:1, v: v: v) and washed at 75°C for 15 min. The electrode was then transferred to 2 mL of CP-1 (0.5 mM) solution for 12 h, followed by immersion in 2 mL of 2-mercaptoethanol (0.5 mM) solution for 4 h. The electrode was washed with Milli-Q water and ethanol then blown dry with N_2. The modified gold electrode was used as the working electrode, saturated Ag/AgCl electrode as the reference electrode and the platinum wire electrode as the counter electrode. 0.1 M TBS containing 5 mM $K_3[Fe(CN)]_6$ and $K_4[Fe(CN)]_6$ was used as the base solution for the preparation of different concentrations of DG12 solution. Experimental parameters: mode selection “IMP-A.C. impedance”, open-circuit potential 0.3 V, alternative voltage 5 mV,

frequency range: 100 kHz–0.1 Hz, EIS data were recorded after 5 min immersion in DG12 solution. The impedance spectra were plotted as Nyquist plots and the charge transfer resistance (R_{ct}) values were obtained in ZView 2 software using an equivalent circuit fit.[8]

Section 2.7 QCM-D measurements

QCM-D experiments were used to study the adsorption dynamics.[9] The QCM-D (Q-Sense E4 system, Biolin Scientific Corp., Sweden) quartz crystal (QC) resonator chip (14 mm diameter, frequency 4.95 ± 0.05 MHz) was cleaned in the same way. All QCM-D experiments were performed at 25°C. The channels and tubes were cleaned with ultrapure water and dried in N_2 before testing, then the functionalized gold chip was mounted in a flow cell for frequency and dissipation measurements. After stabilizing the basic resonance frequency with ultrapure water and TBS (5 mM, pH 8.0), respectively, the CP-1 solution (1 mM) was modified on the chip online, and TBS was added after the frequency was basically stable. Rinse until the curve is stable, then pump DG12 or NSP-1 solution (1 mM) into the flow cell to observe the frequency drop, and then pump TBS to rinse again after the resonance frequency is basically stable. All frequency and dissipation curves over time were recorded by Q-Sense software and analyzed by Q-Tools.

Section 2.8 Isothermal titration microcalorimetry (ITC) experiments

ITC analysis[10, 11] was employed to investigate the interaction of CP-1 with DG12. The experiment was performed by PEAK-ITC at 25 ºC. The CP-1 (5 mM) and two kinds of 12-peptides (0.25 mM) were dissolved in Milli-Q water sufficiently to prepare the work solutions. CP-1 solution was loaded into the syringe and titrated into the calorimetric cell containing DG12 solution. The reference cell was filled with Milli-Q water. The titration sequence consisted of a single 0.4 μL injection followed by a series of 2 μL solution, with a time interval of 120 s between injections to ensure that the thermal power returns to the baseline before the next injection. The stirring speed was 750 rpm. CP-1 and NSP-1 were tested under the same conditions. The exothermic heat value was analyzed by using Origin7.0 software package (OriginLab, Northampton, MA). CP-1 has multiple identical binding sites for DG12. The obtained association constants could be adequately used for the qualitative analysis and comparison of the binding of CP-1 with DG12 or NSP-1.

Section 2.9 CV measurements

Three electrodes system: glassy carbon electrode as working electrode, platinum wire electrode as counter electrode, saturated Ag/AgCl electrode as reference electrode, supporting electrolyte: 5 mM TBS (pH 8.0), experimental parameters: mode selection CV-Cyclic Voltammetry, Init E –2.7 V, Final E 2 V, scan rate 0.05 $V \cdot s^{-1}$, sample interval 1 mV, quite time 2 s. The electrode was placed in CP-1 solution (1 mM) to obtain C-V image, followed by the addition of 1 μM DG12 and mixing to obtain a new C-V spectrum.

Section 2.10 Biolayer interferometry (BLI) measurements

Before the test, dissolve EDC/NHS in Milli-Q water to activate the carboxyl group on the surface of biosensor (amine reactive 2nd generation, AR2G) for 1.5 h, and react with the amino group on CP-1 (3 $mg \cdot mL^{-1}$) for 12 h for coupling, followed by careful washing of unreacted material on sensor surface with TBS (5 mM, pH 8.0). The interaction between CP-1 and DG12 was measured by using an Octet K2 system (Molecular Devices, LLC., USA). A series of DG12 solutions were prepared in TBS, and CP-1 modified biosensor was exposed to different concentrations of DG12 solution, then dissociated in water (pH 4.0). The preparation of sensors and analysis of the interactions were carried out at 25°C. Analysis of the data and determination of equilibrium constant (K_D) were performed on fortebio (Data Analysis 11.0).

Section 2.11 Electroosmotic flow (EOF) experiments

EOF is an electrokinetic phenomenon that occurs when an ion flow passed through a channel that contains excess surface charge.[12-14] EOF rate is obtained by measuring the flux of neutral probe molecule (e.g., phenol) through nanochannels. The feed chamber at the tip side is filled with TBS (5 mM, pH 8.0) solution containing 10 mM phenol, while the permeate chamber has only TBS, and a constant voltage of 2 V is applied through a pair of platinum wire electrodes with the anode in the feed solution, driving the phenol from the feed to the permeate. Phenol absorbance was first measured in the permeate chamber before and after voltage application for the unmodified PET nanochannels with CP-1, then phenol absorbance was measured in the permeate chamber before and after voltage application for the nanochannels modified with CP-1, and finally CP-1 nanochannels were periodically assayed for phenol in the permeate before and after voltage application to the permeate chamber after interaction with DG12. Phenol

absorbance was measured by UV−Vis detector and phenol molarity (absorbance) - time was plotted. The surface charge density of nanochannels in the three different states was calculated respectively.

Section 2.12 ^{1}H–^{1}H NMR experiments

Two-dimension NMR spectra were used to study the interaction between CP-1 and DG12 at 25°C with DMSO-d_6 as solvent. ^{1}H, ^{13}C, ^{13}C–^{1}H (heteronuclear singular quantum correlation) HSQC, and ^{1}H–^{1}H (correlation spectroscopy) COSY NMR experiments were performed to investigate the binding details.[15] ^{1}H–^{1}H correlation NMR spectra of CP-1 and DG12 at a concentration of 20 mM were first measured, followed by mixing the equimolar concentration of CP-1 and DG12 and testing under the same conditions.

Section 2.13 Molecular docking

The DG12 and CP-1 were docked by using the AutoDock 4. 2.[16] DG12 model was created according to the percentage secondary structure contents determined (Fig. S22), semi-flexible docking was performed, and the binding model with the minimum energy was selected through the scoring function. Molecular docking includes molecular preprocessing, molecular docking and analysis. We adopted a blind approach (no active site defined) and the maximum number of conformation was set to 20 conformations. We identified the best binding model from hundreds of models generated by multiple docking experiments, and performed detailed interaction analysis, subsequently.

Section 2.14 FT-IR experiments

IR spectra were recorded on a Bruker Vertex 80v FT-IR spectrometer in attenuated total reflection (ATR) mode. CP-1 (1 mM) and DG12 (1 mM) were dissolved in water and stirred for one hour, then lyophilized to obtain a solid powder.[17] The ATR crystal was washed with ultrapure water and ethanol before each measurement, then the solid powder samples of CP-1, DG12 and the mixture were recorded on the spectrometer in 1200 scans in ATR mode in turn.

Section 2.15 Enzymatic digestion reaction

Before testing[18] we prepared 50 mM TBS (pH 8.0) of RanGTPase activating protein 1 (RanGAP1) peptide and then prepared TBS containing SUMO-specific protease 1 (SENP1) at

10:1 (m: m) of protein: enzyme, adding SUMOylated RanGAP1 solution (1 μM) to the electrolytic cell first, then adding SENP1 solution when the current is constant, the current signals were recorded continuously. The solution was lyophilized and desalted before and after the reaction, 0.5 μL of the analyte and 0.5 μL of CHCA substrate (α-cyano-4-hydroxycinnamic acid, 7 $mg \cdot mL^{-1}$, dissolved in 60% CAN solution containing 0.1% tetrafluoroacetic acid) were spotted sequentially on the MALDI target plate. MS analysis was performed by using the solid-state laser SmartBean technology (355 nm) and positive ion reflection mode.

Section 2.16 Immunofluorescence

Cells were fixed in 4% formaldehyde for 10 minutes at room temperature, permeabilized in PBS supplemented with 0.5% Triton X-100 for 10 minutes and then incubated with 1% BSA and 22.52 $mg \cdot mL^{-1}$ glycine in PBST (PBS + 0.1% Tween 20) for 30 min to block the non-specific binding. Immunostaining was performed for two hours at room temperature using rhodamine-labelled CP-1 or anti-SUMO1 antibody (Abcam, cat#ab32058). Cells incubated with anti-SUMO1 antibody were washed 3 times with PBS and incubated with FITC*Goat Anti-Rabbit IgG (Immunoway, cat#RS0004) for one hour at room temperature. Cells were incubated with 1 $\mu g \cdot mL^{-1}$ DAPI staining for 5 minutes. Fluorescent signals were detected at room temperature using a confocal microscope.

Section 3. Supplementary Schemes, Figures and Tables

Table S1. SENP1 protease in clinical and molecular studies.[19]

Main Localization	Enzymatic Activity	Cancer/RNA Expression	Clinical Studies	Molecular Studies
Nucleoplasm	C-terminal Hydrolase, isopeptidase	Breast	Polymorphism c. 1691+36C＞T (rs12297820) was associated with risk of metastases	
		Colorectal / ↑	Not related to tumor invasion, lymph node involvement or tumor cell differentiation	Regulates cell cycle via CDK inhibitors (p16, p19, p21 and p27)
		Myeloma / ↑		Regulates sensitivity to apoptosis, proliferation, and colony formation regulates NF-κB signaling
		Liver / ↑	Prognostic marker	
		Neuroblastoma / ↑	Overexpressed in metastatic tissues vs. primary tumor tissue	Promotes cell invasion and migration regulates the expression of CDH1, MMP-9, and MMP-2
		Pancreatic / ↑	Correlates with lymph node metastasis and TNM stage	Up-regulates MMP9
		Prostate / ↑	Correlates with cancer aggressiveness and recurrence	Androgen receptor and hypoxia-induced stabilization of H1F1α and overexpression of downstream proteins (MMP2/MMP9)
		Renal / ↑	Prognostic marker	

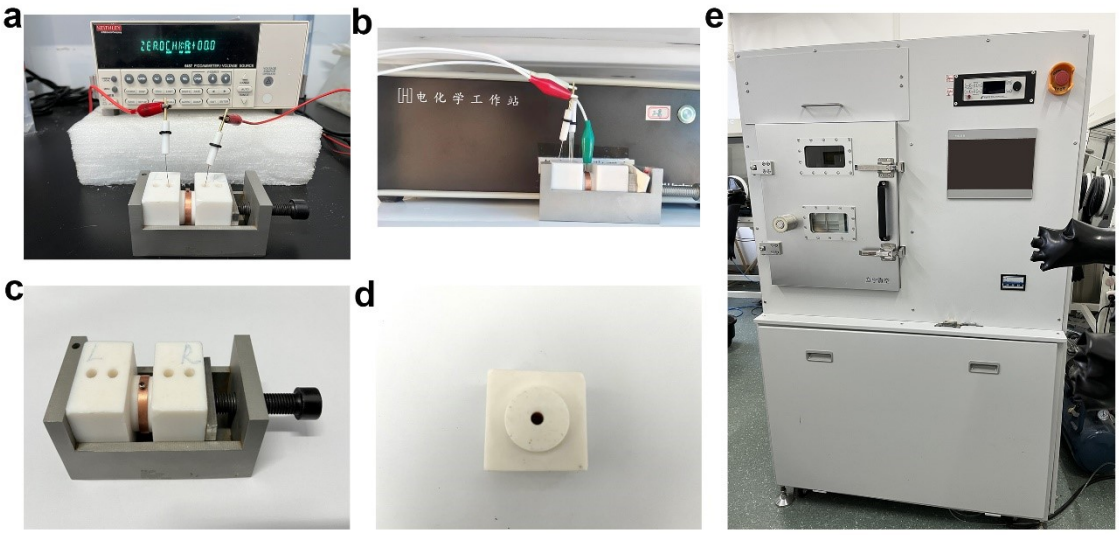

Scheme S1. (a) Etching and measuring nanochannels transmembrane ionic current by using a Keithlay 6487 picoammeter. (b) Measurement of Faraday current by using a CHI 760E electrochemical workstation. (c) Home-made stainless steel with a pair of Teflon modules and a copper piece. (d) The modules have an internal diameter of 5 mm. (e) Coater for nickel and gold plating of PET films.

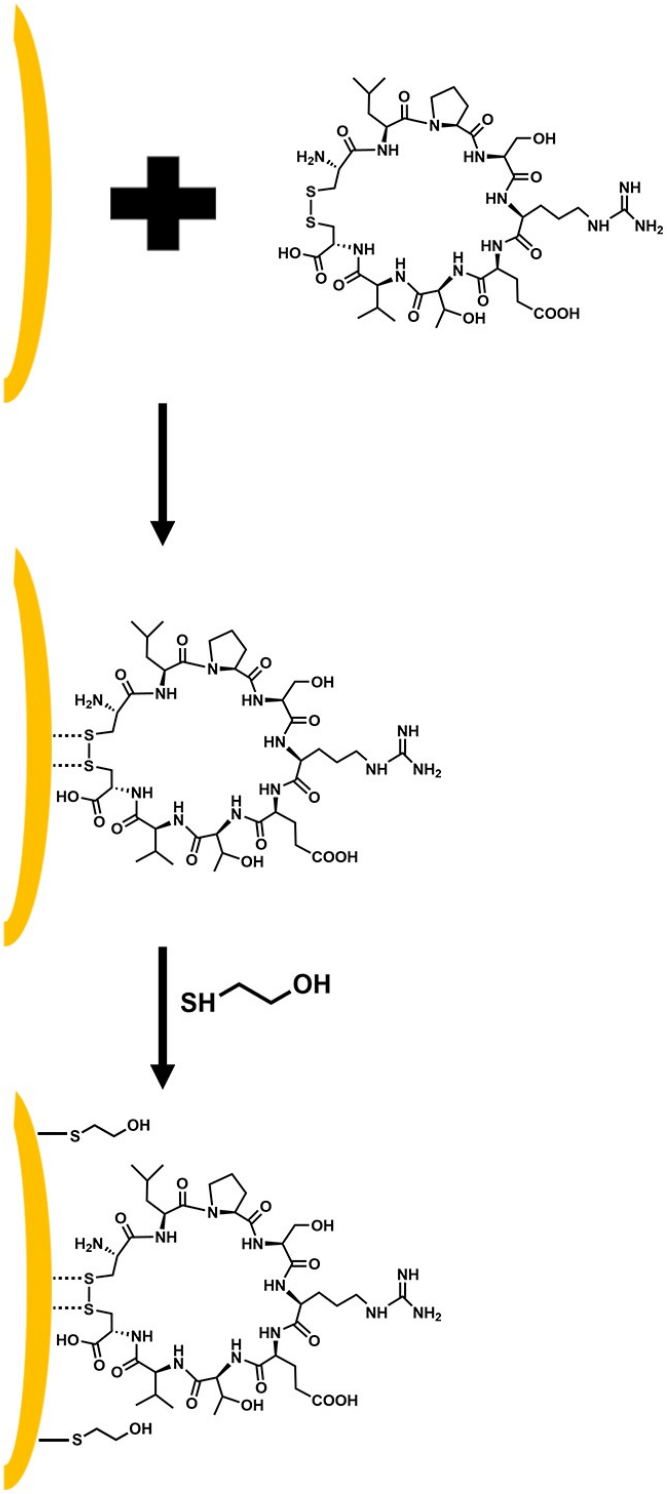

Scheme S2. Preparation of CP-1 modified PET nanochannels. S-S bond can be anchored to the gold layer, then combine 2-mercaptoethanol with gold film to reduce non-specific adsorption.

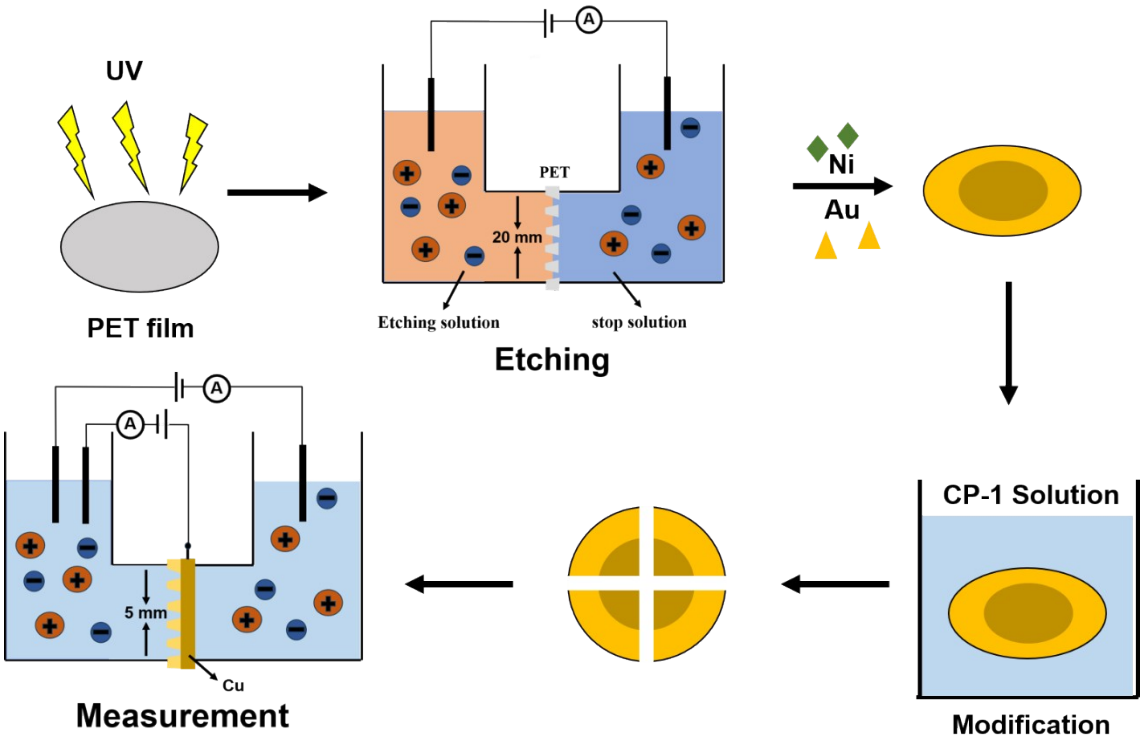

Scheme S3. (a) Implementation processes of the nanochannel device including preparation, etching, nickel/Au plating, modification, cutting, and ionic current/Faraday current measurement.

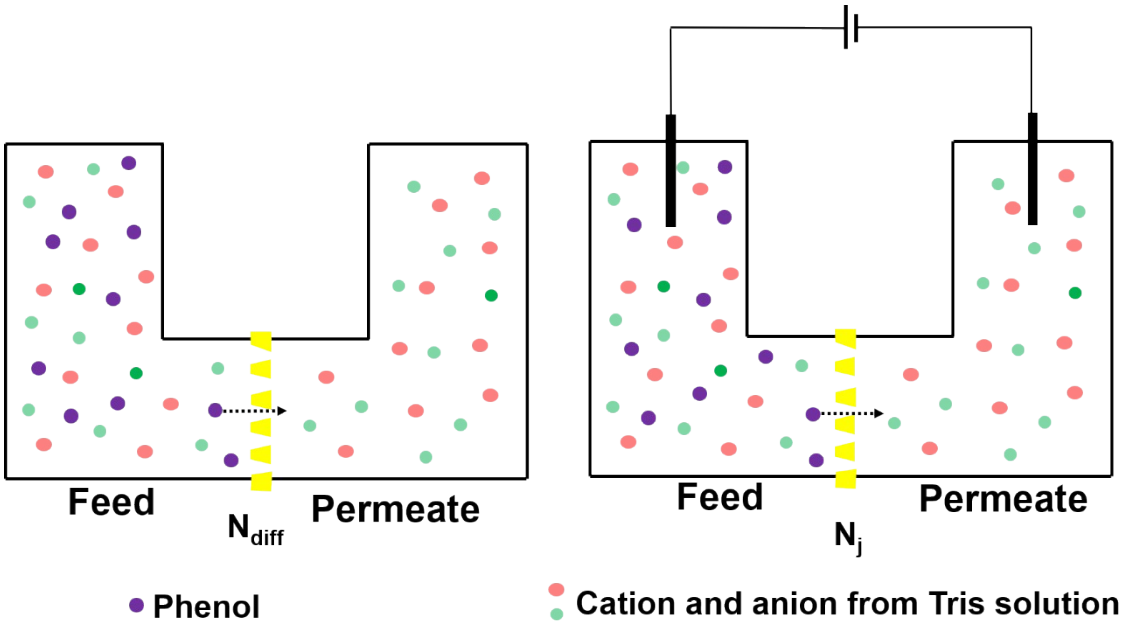

Scheme S4. EOF measurements. The surface charge density of nanochannels in three different states was calculated by measuring the rate of phenol permeation through PET film before and after voltage application.

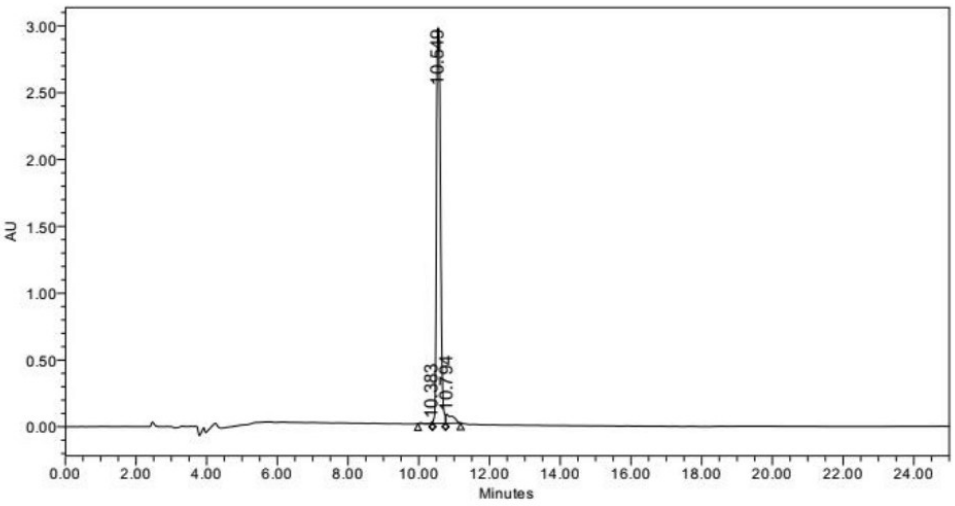

	RT	Area	% Area	Height
1	10.383	73702	0.30	8647
2	10.549	23498256	95.75	2960043
3	10.794	970170	3.95	65830

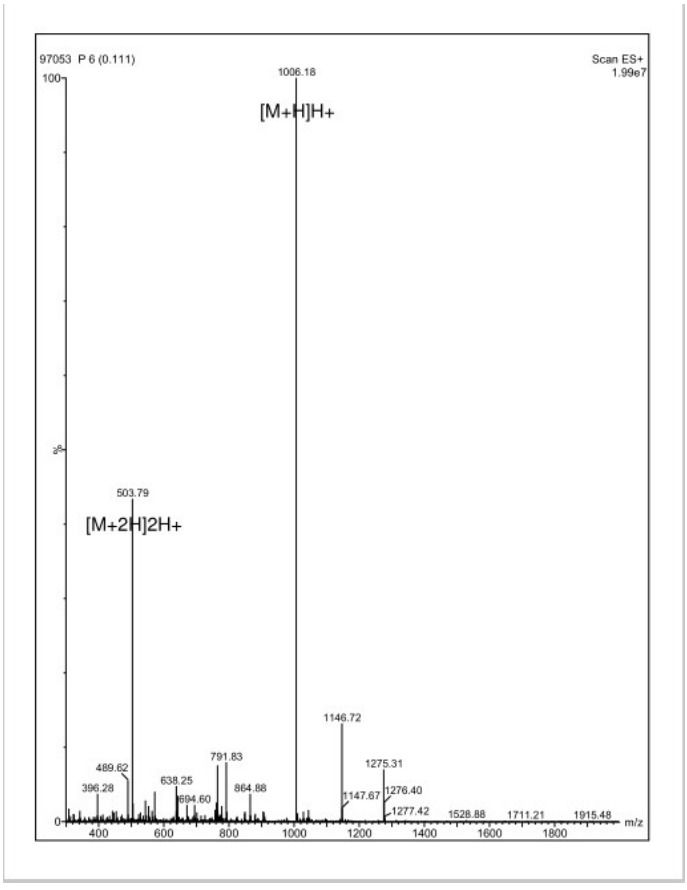

Figure S1. HPLC and mass spectrometry analysis of CP-1.

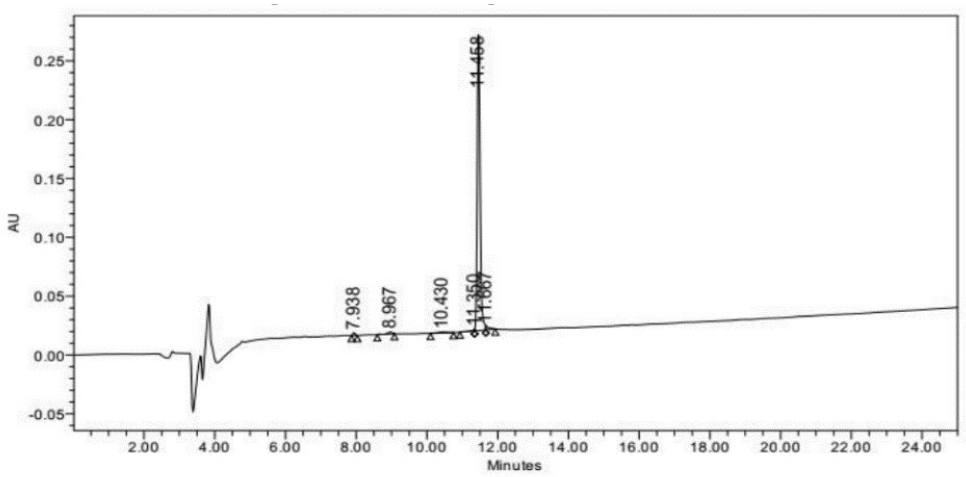

	RT	Area	% Area	Height
1	7.938	10283	0.69	2218
2	8.967	15181	1.02	1745
3	10.430	15416	1.03	746
4	11.350	8098	0.54	1394
5	11.458	1422980	95.31	253480
6	11.667	21099	1.41	3299

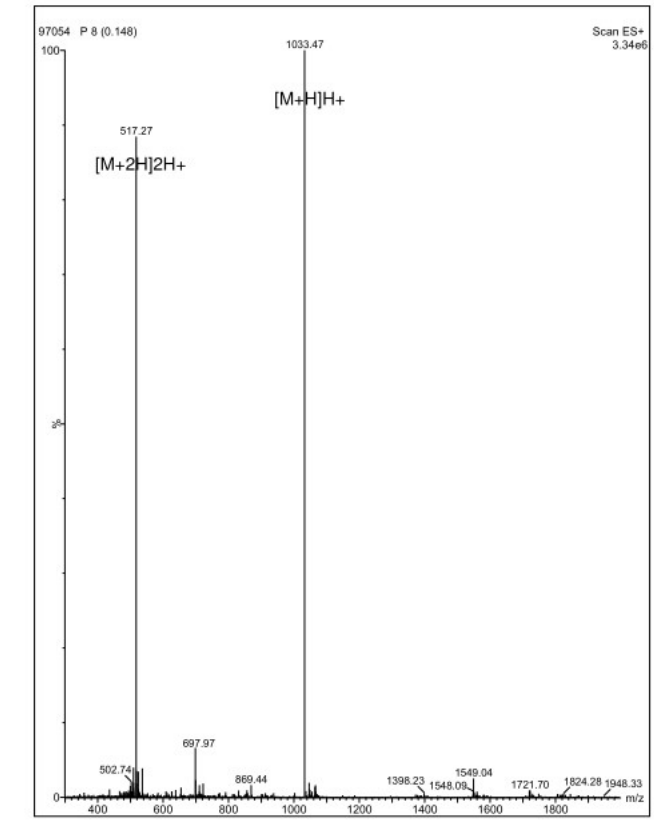

Figure S2. HPLC and mass spectrometry analysis of CP-2.

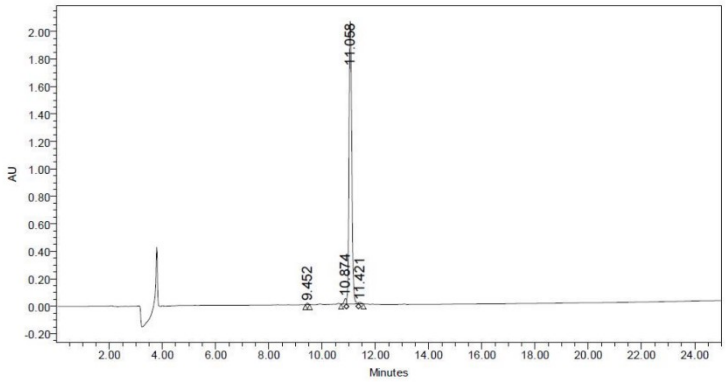

	RT	Area	% Area	Height
1	9.452	50391	0.33	9708
2	10.874	229722	1.52	40543
3	11.058	14789982	97.69	2084842
4	11.421	69950	0.46	10610

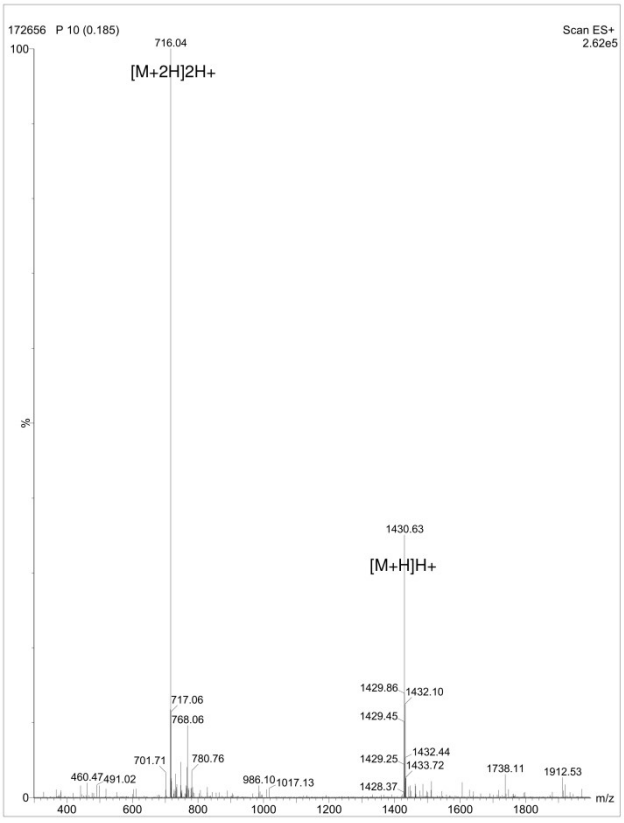

Figure S3. HPLC and mass spectrometry analysis of rhodamine-labeled CP-1.

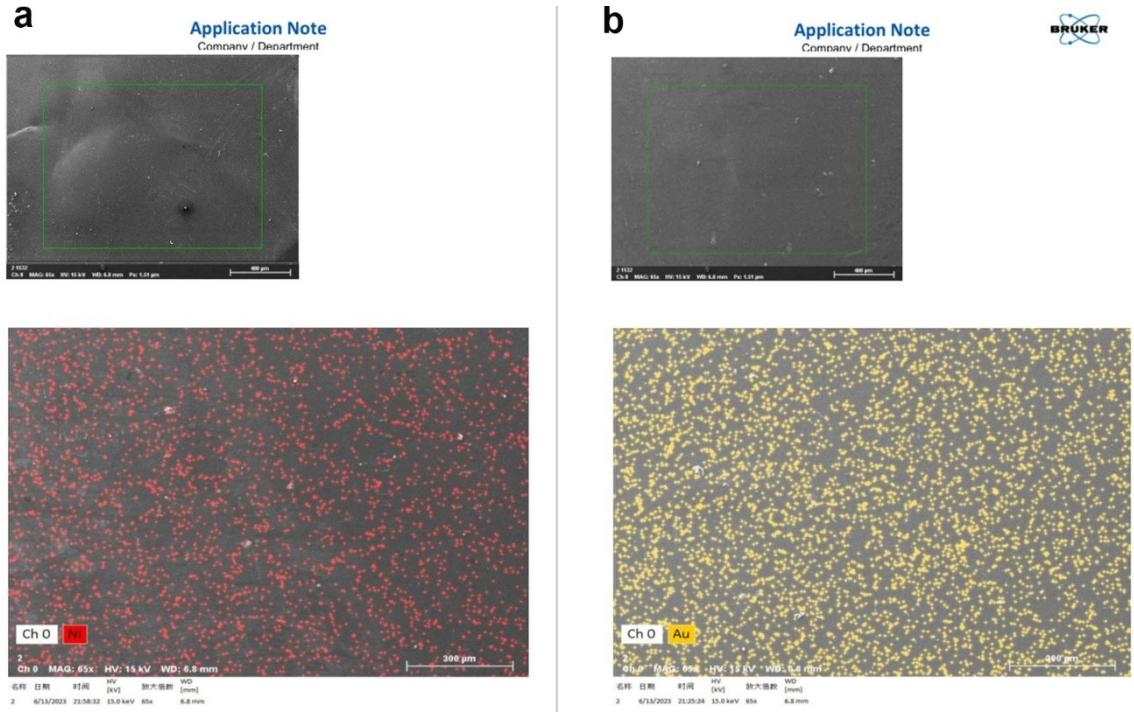

Figure S4. Distribution of (a) nickel layer and (b) gold layer on PET film as observed by SEM.

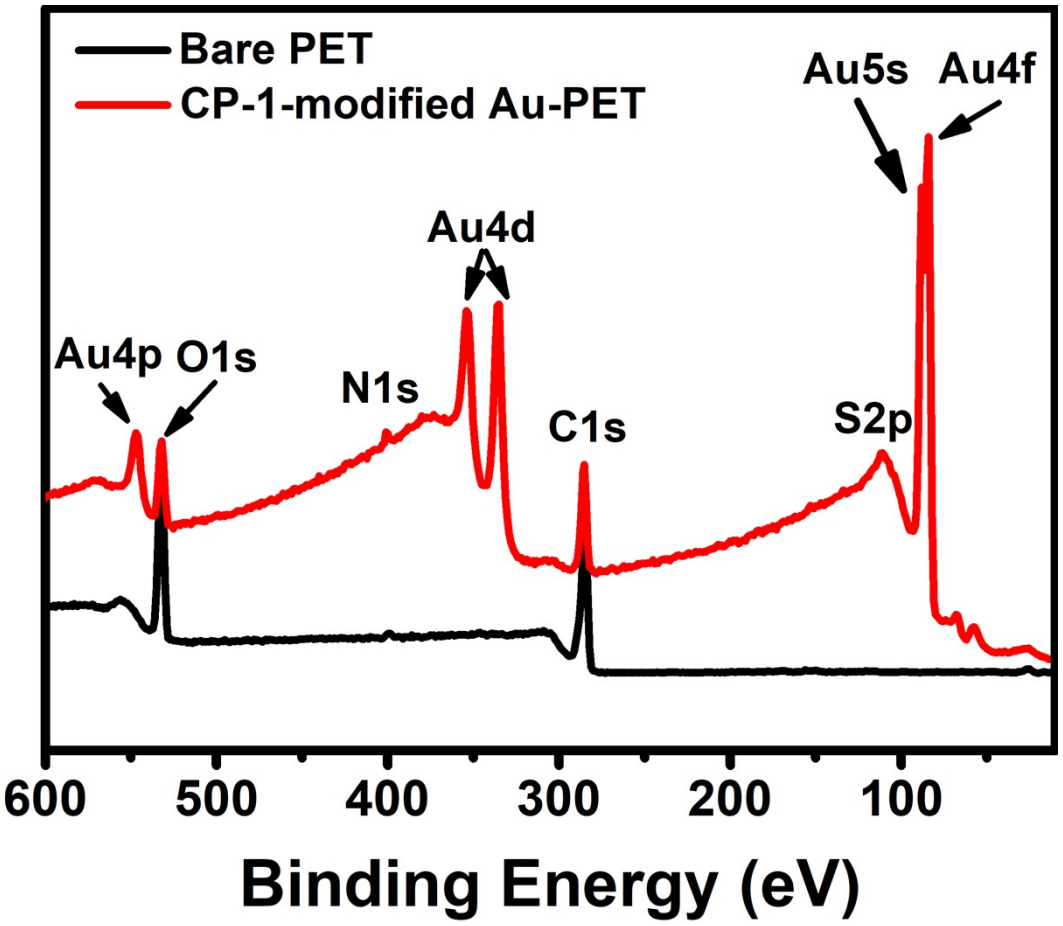

Figure S5. In XPS wide scan spectra, the CP-1 modified PET film (red) exhibits elevated N1s peaks and new S2p peaks, as well as multiple energy peaks for gold, in contrast to the bare PET nanochannel film (black).

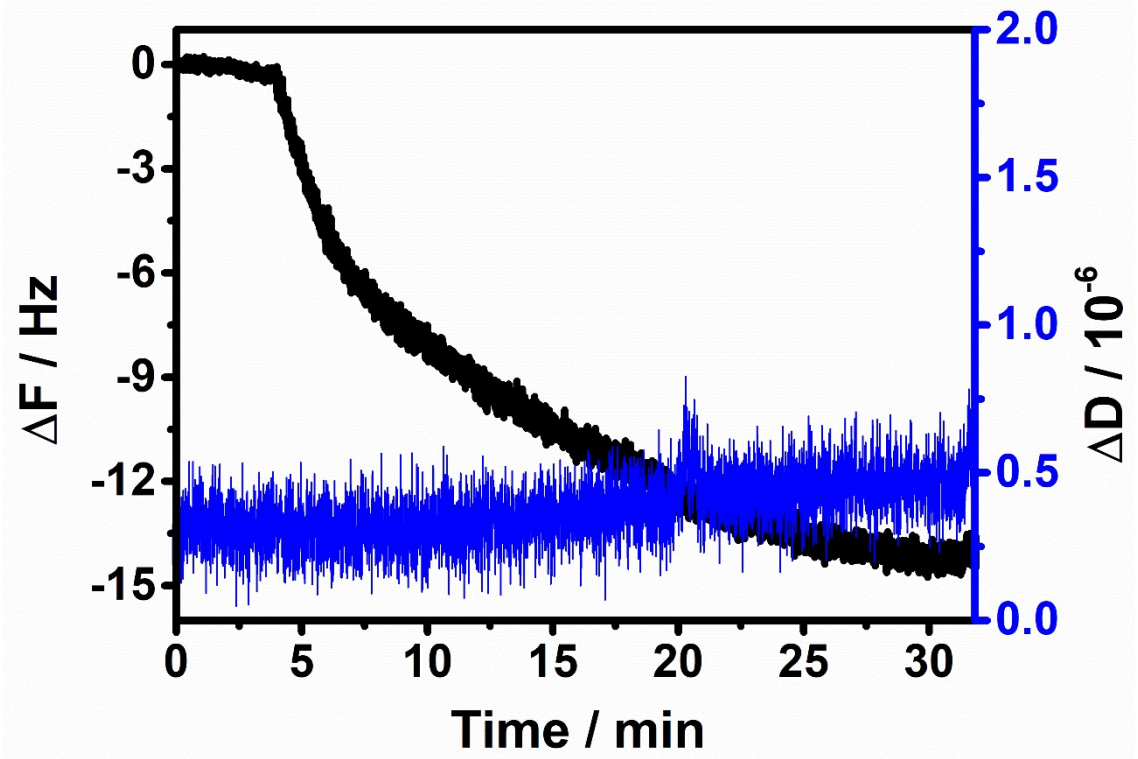

Figure S6. The frequency variation and energy dissipation curves of CP-1 (1 mM) modified online by QCM-D experiment were carried out at 25°C.

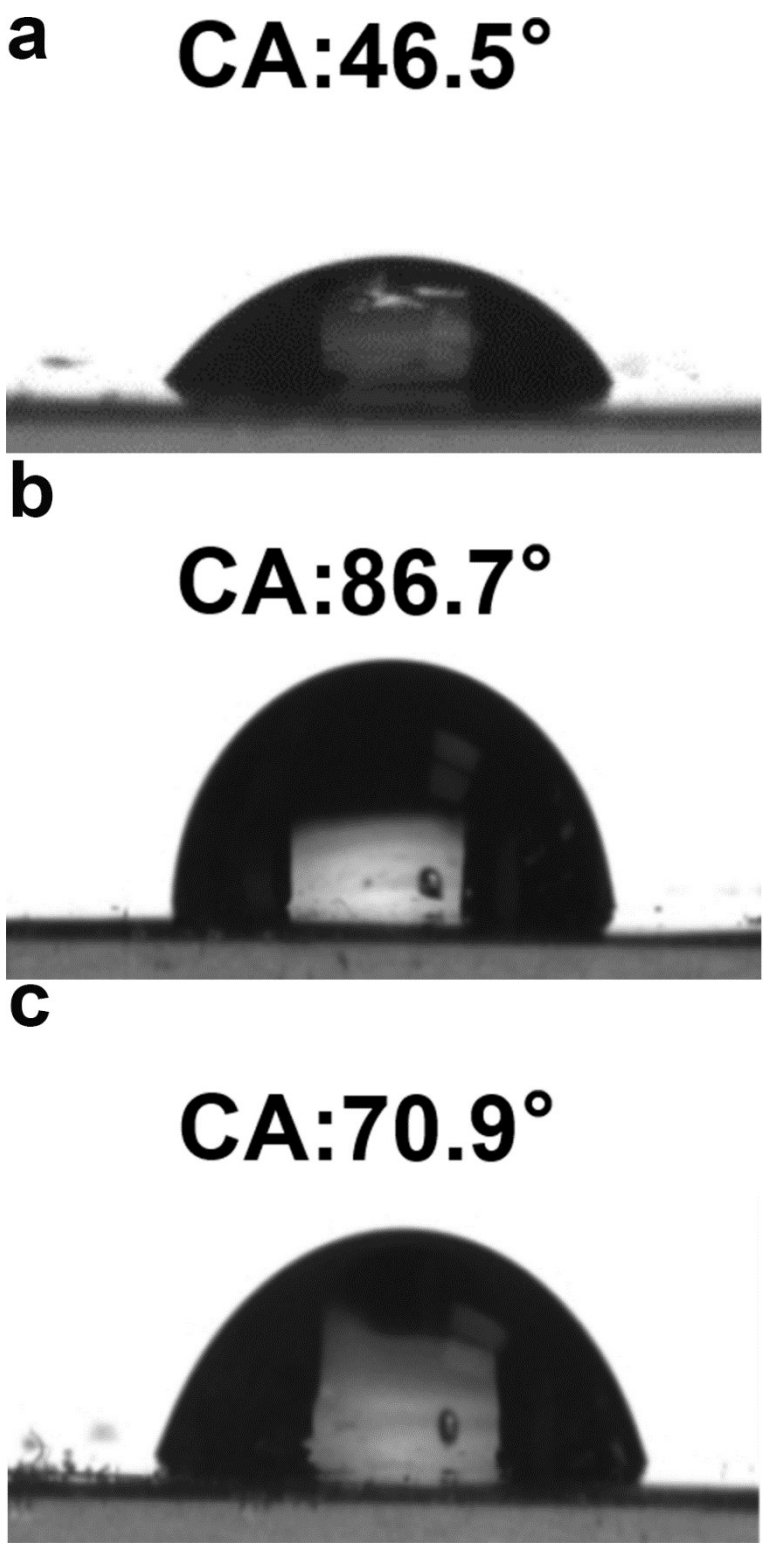

Figure S7. The CA of PET film (a), metalized PET film (b) and CP-1 modified PET film (c) were 46.5°, 86.7° and 70.9°. This experiment was finished at ambient temperature with almost 10 μL water drops onto the sample surface.

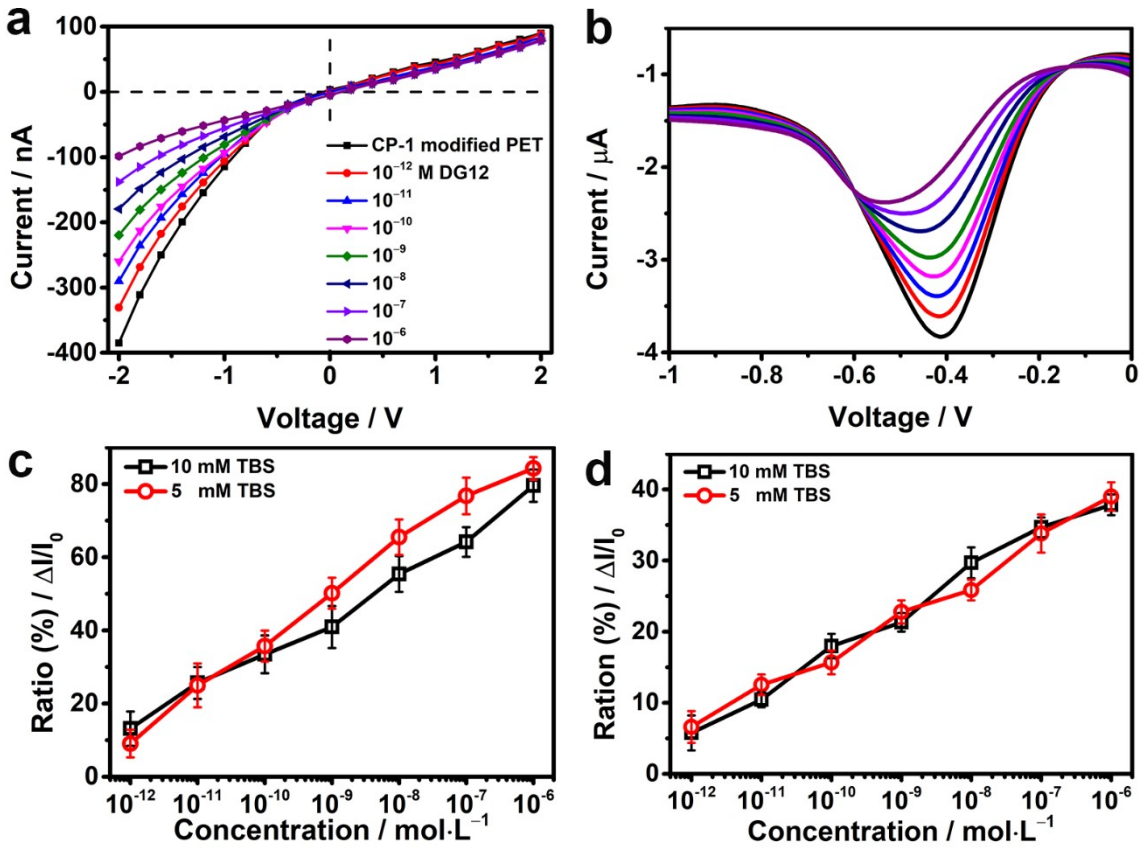

Figure S8. Transmembrane ionic current curves (a) and Faraday current curves (b) of CP-1-modified nanochannels in response to the addition of different concentrations of DG12 in TBS (10 mM; pH 8.0) at 25°C. Concentration-dependent transmembrane ionic current increase ratios ($\Delta I/I_0$) (c) and Faraday current increase ratios ($\Delta I/I_0$) (d) of CP-1-modified nanochannels in response to DG12 in 10 Mm (black) or 5 mM (red) TBS at 25°C.

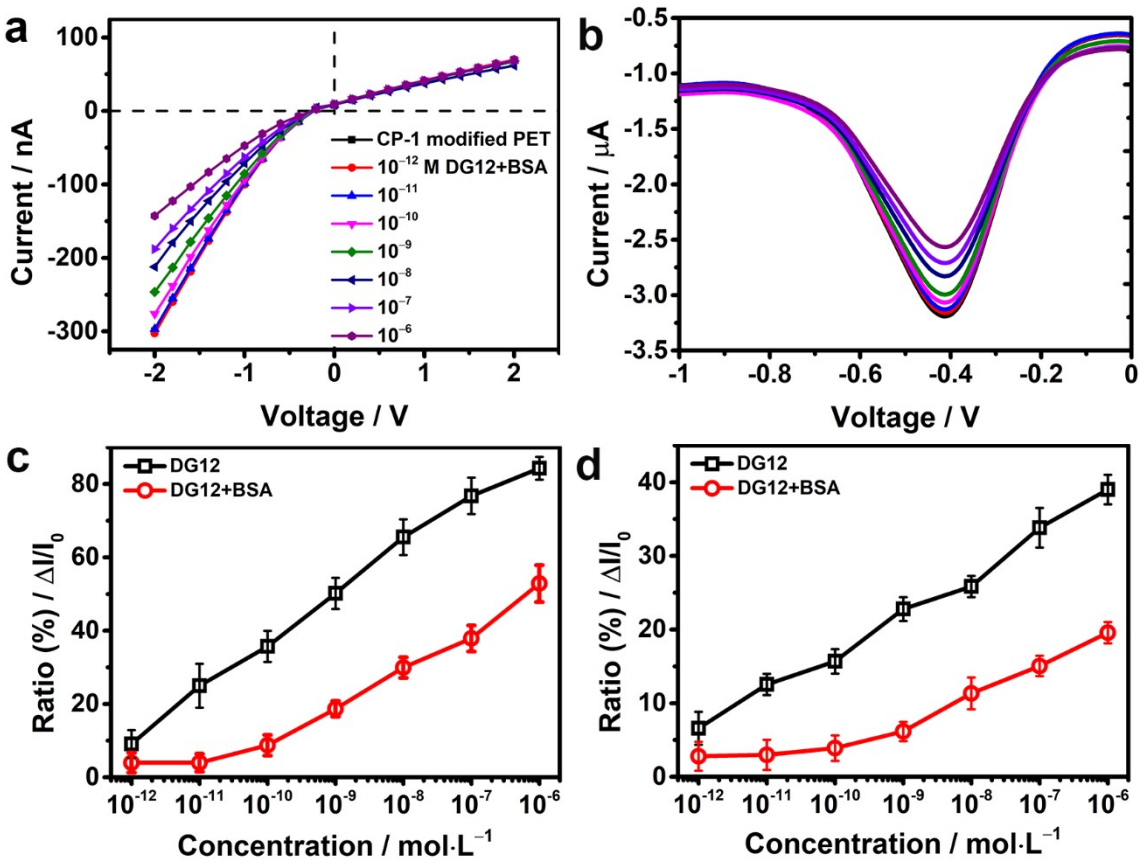

Figure S9. Transmembrane ionic current curves (a) and Faraday current curves (b) of CP-1 modified nanochannels on 10 μM of tryptic digests BSA containing different concentrations of DG12 in TBS (5 mM, pH 8.0).

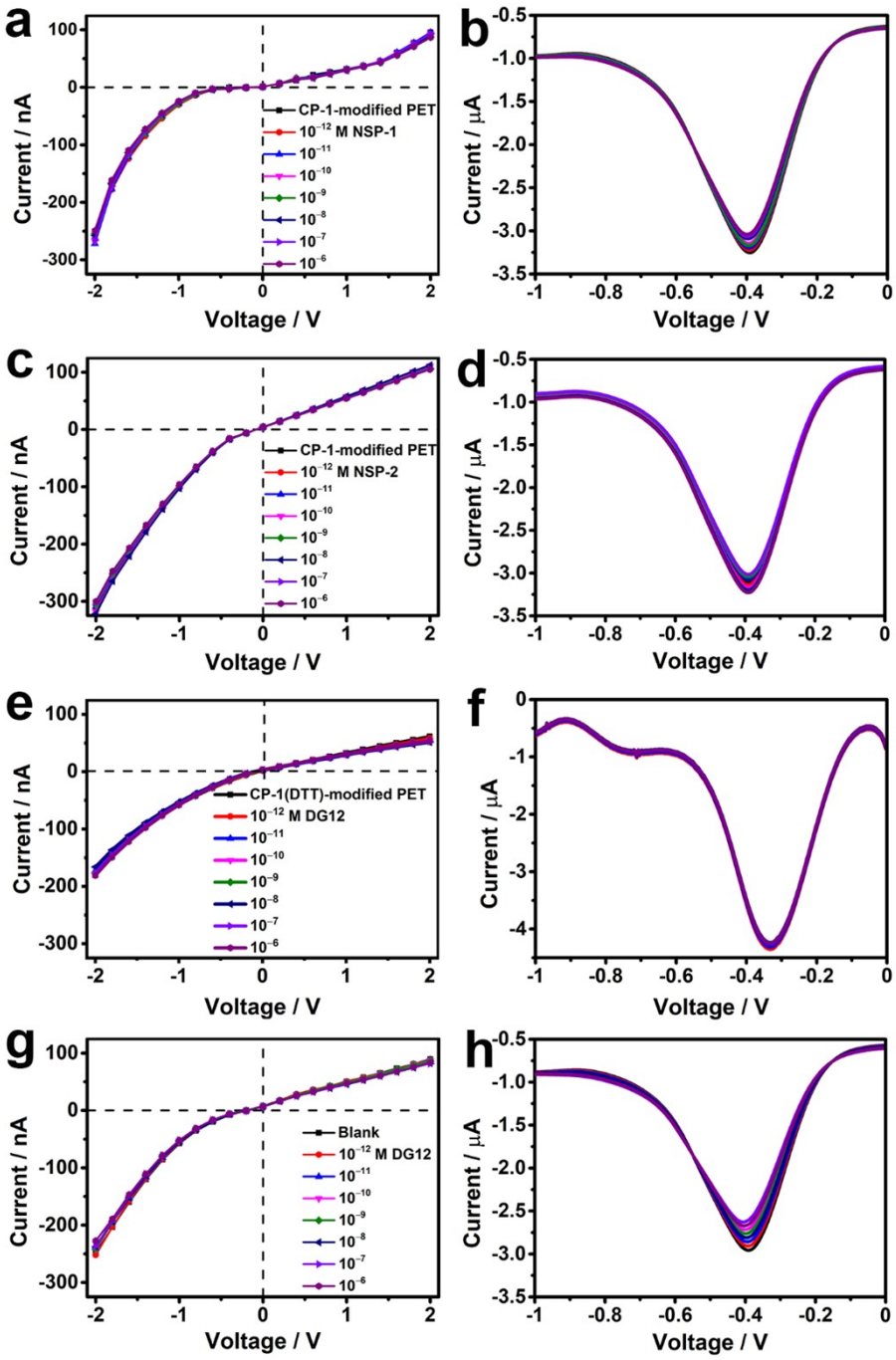

Figure S10. Transmembrane ionic current curves (a, c, e, g) and Faraday current curves (b, d, f, h) of CP-1 (a, b, c, d), DTT-treated CP-1 (e, f) or Blank (g, h)-modified nanochannels in response to addition of different concentrations of NSP-1 (a, b), NSP-2 (c, d) or DG12 (e, f, g, h) in TBS (5 mM, pH 8.0) at 25 °C.

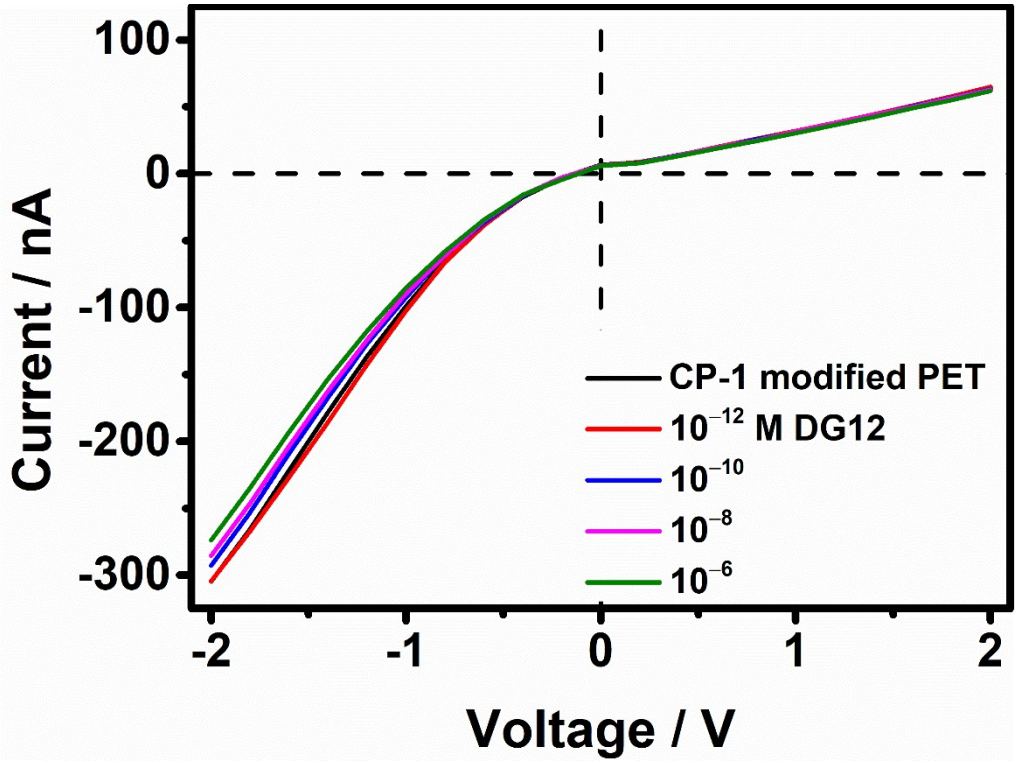

Figure S11. I–V curves of non-metallized PET film chemically modified with CP-1 and recognition of different concentrations of DG12 in TBS (5 mM, pH 8.0) at 25 °C.

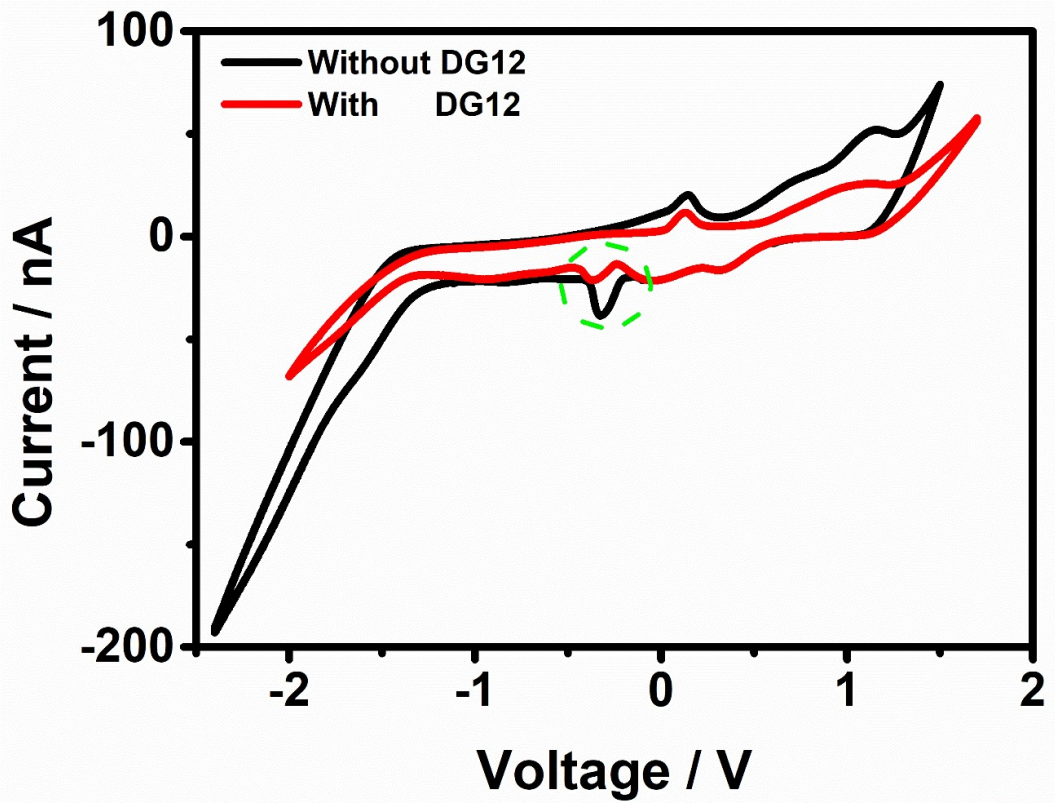

Figure S12. CV image of CP-1 (1 mM) in TBS (black) and after addition of DG12 (1 μM) (red) in the buffer solution of 10 mM Tris-HCl + 500 mM KCl (pH 8.0), the scan rate is 0.05 $V \cdot s^{-1}$. Green dashed circle indicates the decrease of the reduction peak.

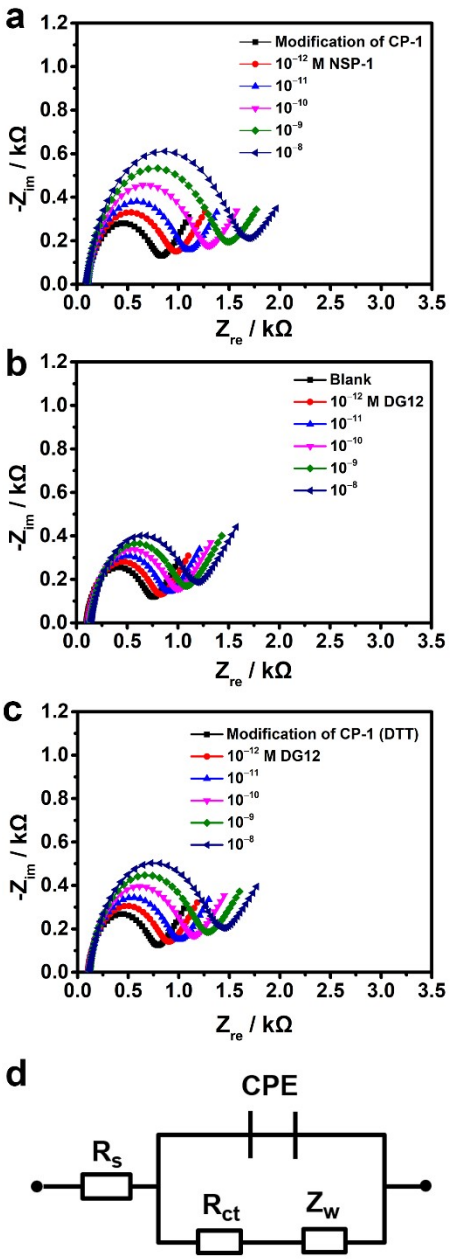

Figure S13. The corresponding impedance spectra (Nyquist plots) of (a) CP-1 (0.5 mM), (b) Blank or (c) DTT-treated CP-1 (0.5 mM) modified gold electrodes in response to the addition of different concentrations of NSP-1 (a) or DG12 (b, c) in 0.1 M TBS containing 5 mM K_3[Fe (CN)]$_6$ and K_4[Fe (CN)]$_6$. (d) Equivalent circuit diagram.

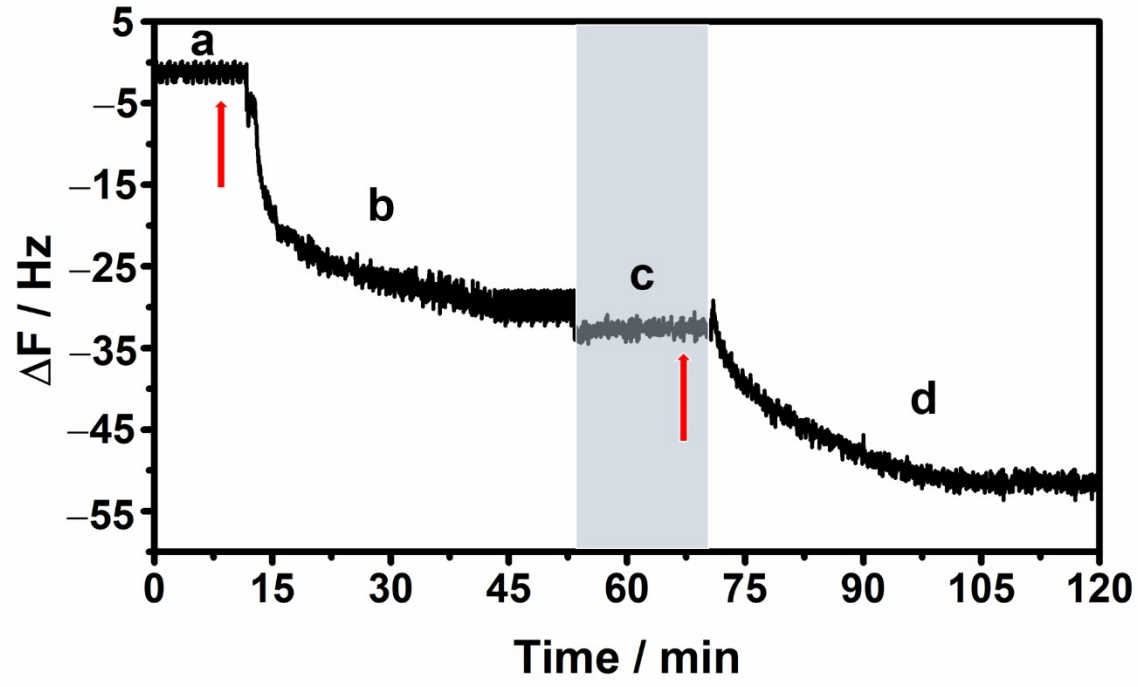

Figure S14. The online modification of CP-1 (1 mM) and the frequency change profile of binding to DG12 (1 mM) were investigated by QCM-D experiments at 25°C. a: rinse with TBS; b: pump in CP-1; c: rinse with TBS; d: pump in DG12.

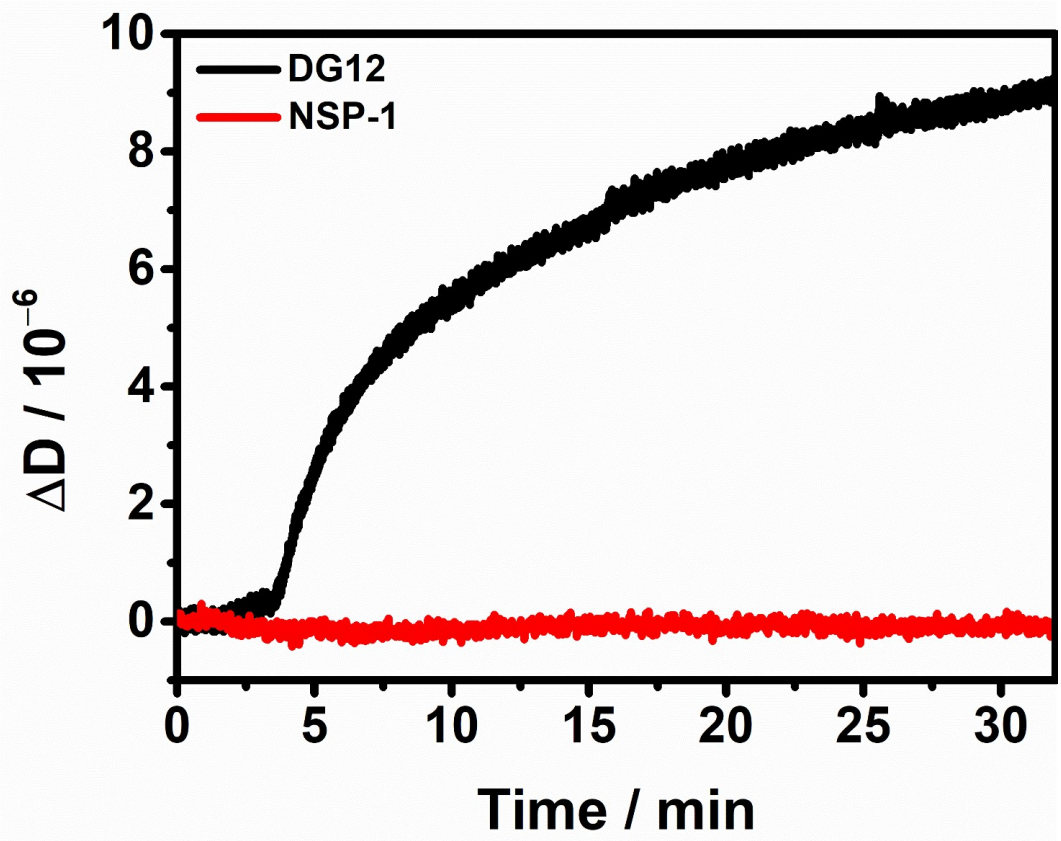

Figure S15. The energy dissipation curves of the CP-1 (1 mM) modified gold chip was tested by QCM-D experiments with 1 mM DG12 (black) and 1 mM NSP-1 (red), respectively, at 25 °C.

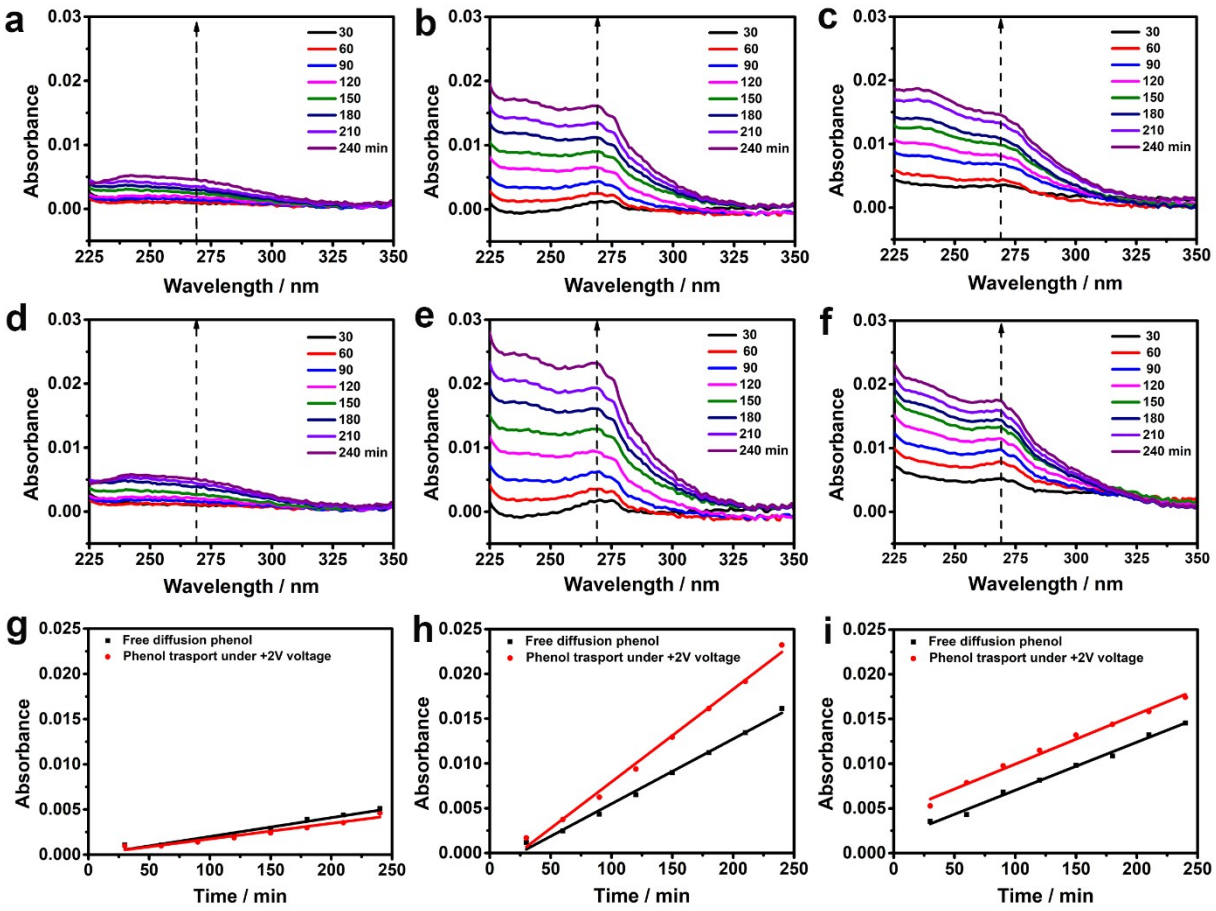

Figure S16. Wavelength-absorbance curves (a, b, c, d, e, f) with (d, e, f) and without (a, b, c) applied voltage of blank (a, d), CP-1 modified (b, e) or DG12 combined CP-1 (c, f)-nanochannels for phenol (10 mM) from feed chamber to permeate chamber in TBS (5 mM, pH 8.0). The fitted phenol transmission curves for blank PET film (g), CP-1 modified PET film (h) and CP-1 modified PET film after bound to DG12 (i) were obtained before and after the applied voltage in the time-absorbance plots.

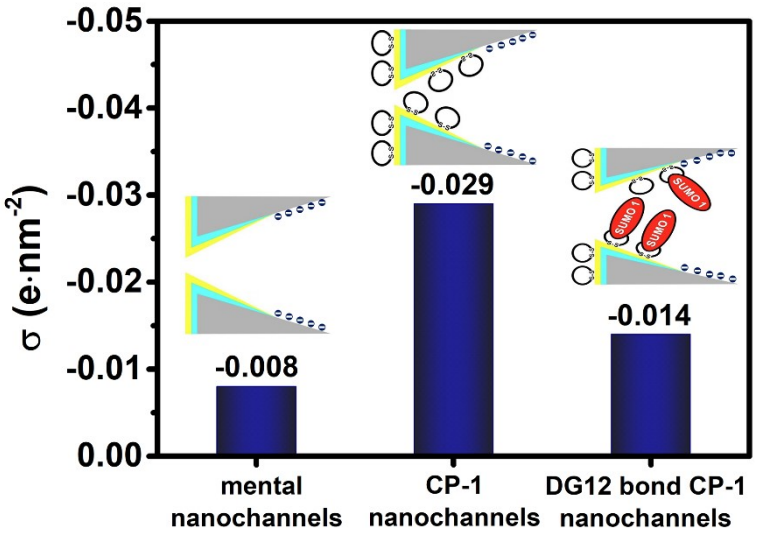

Figure S17. Surface charge density values of three types of nanochannels, which were calculated on the basis of phenol transport rates.

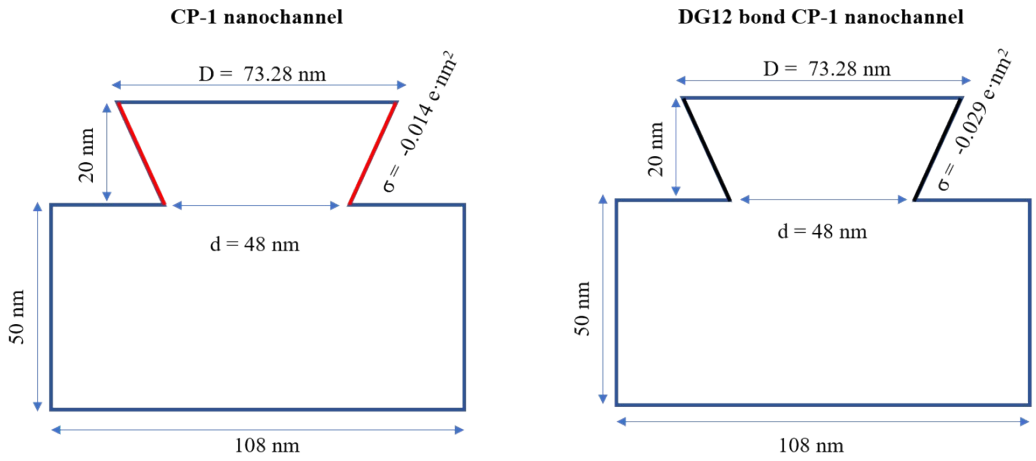

Figure S18. The model of numerical simulation about CP-1 nanochannels and DG12 bond CP-1 nanochannels. The model of nanochannel due to SEM measurement is about 12000 nm (length), 680 nm (base side), and 48 nm (tip side). As only considering the Au-coated area, we set the simulation size as shown in the Figure, 20 nm (length), 48 nm (tip side) and 73.28 nm (base side) proportionally. The reservoirs with a width of 108 nm and a height of 50 nm. The surface charge density of CP-1 nanochannel (–0.029 e·nm^2) and DG12 bond CP-1 nanochannels (–0.014 e·nm^2) are measured by EOF experiments. Applying 2 V potential as a driving force to demonstrate the ion transport properties under experimental conditions.

Finite-element simulation of ion concentration distribution

The finite-element computations were performed using COMSOL Multiphysics 5.4 on the Poisson and Nernst-Planck equations:

$$J_i = D_i\left(\nabla c_i + \frac{z_i F c_i}{RT}\nabla\varphi\right) + uc_i \quad (1)$$

$$\nabla^2\varphi = -\frac{F}{\varepsilon}\sum z_i c_i \quad (2)$$

$$\nabla \cdot J_i = 0 \quad (3)$$

$$\underset{n}{\rightarrow} \cdot \nabla\varphi = -\frac{\sigma}{\varepsilon} \quad (4)$$

$$\underset{n}{\rightarrow} \cdot J_i = 0 \quad (5)$$

Equation (1) is the Nernst–Planck equation that describes the transport property of a charged nanochannel. The electric potential and ionic concentration can be characterized by Equation (2). Besides, the flux should satisfy the time-independent continuity when the system reaches a stationary regime (Equation (1)). The physical quantities J_i, D_i, c_i, φ, u, R, T and ε refer to the ionic flux, diffusion coefficient, Faraday constant, absolute temperature, and dielectric constant of the electrolyte solutions, respectively. The coupled equations can be solved by assuming appropriate boundary conditions. The boundary condition for potential φ on the channel wall is Equation (4); and the ionic flux has zero normal components at boundaries (Equation (5)), where σ represents the surface charge density and is given by the EOF experiment. Electrolyte solution was 100 mM KCl, the diffusion coefficients of K^+ and Cl^- were set as $1.96 \times 10^{-9} \cdot m^2 \cdot s^{-1}$ and $2.03 \times 10^{-9} \cdot m^2 \cdot s^{-1}$, respectively. The simulated model is shown in Figure S18.

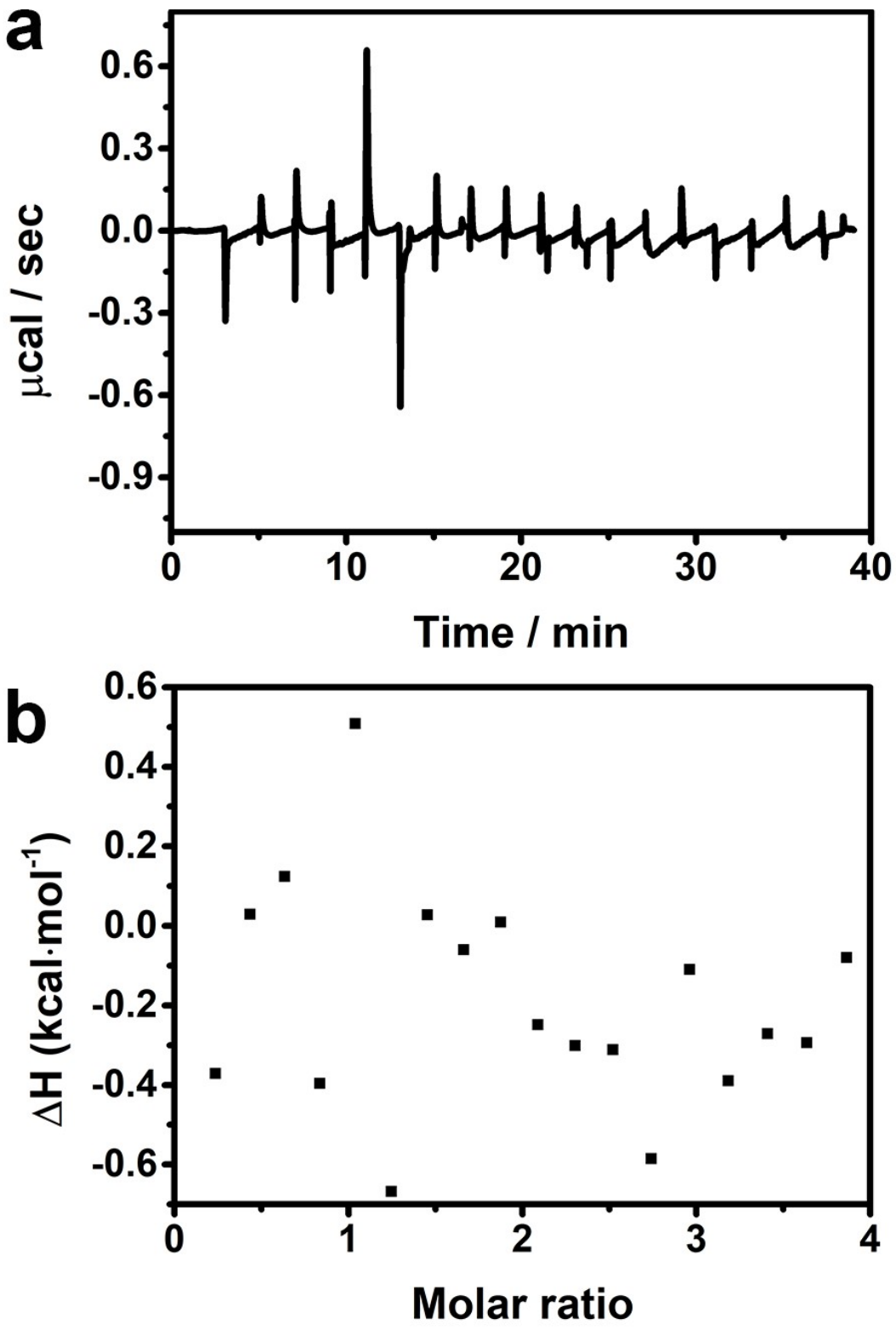

Figure S19. ITC raw data. The corresponding fitting curve of CP-1 upon successive titration

of (a) NSP-1 and (b) non-linear fitting curve.

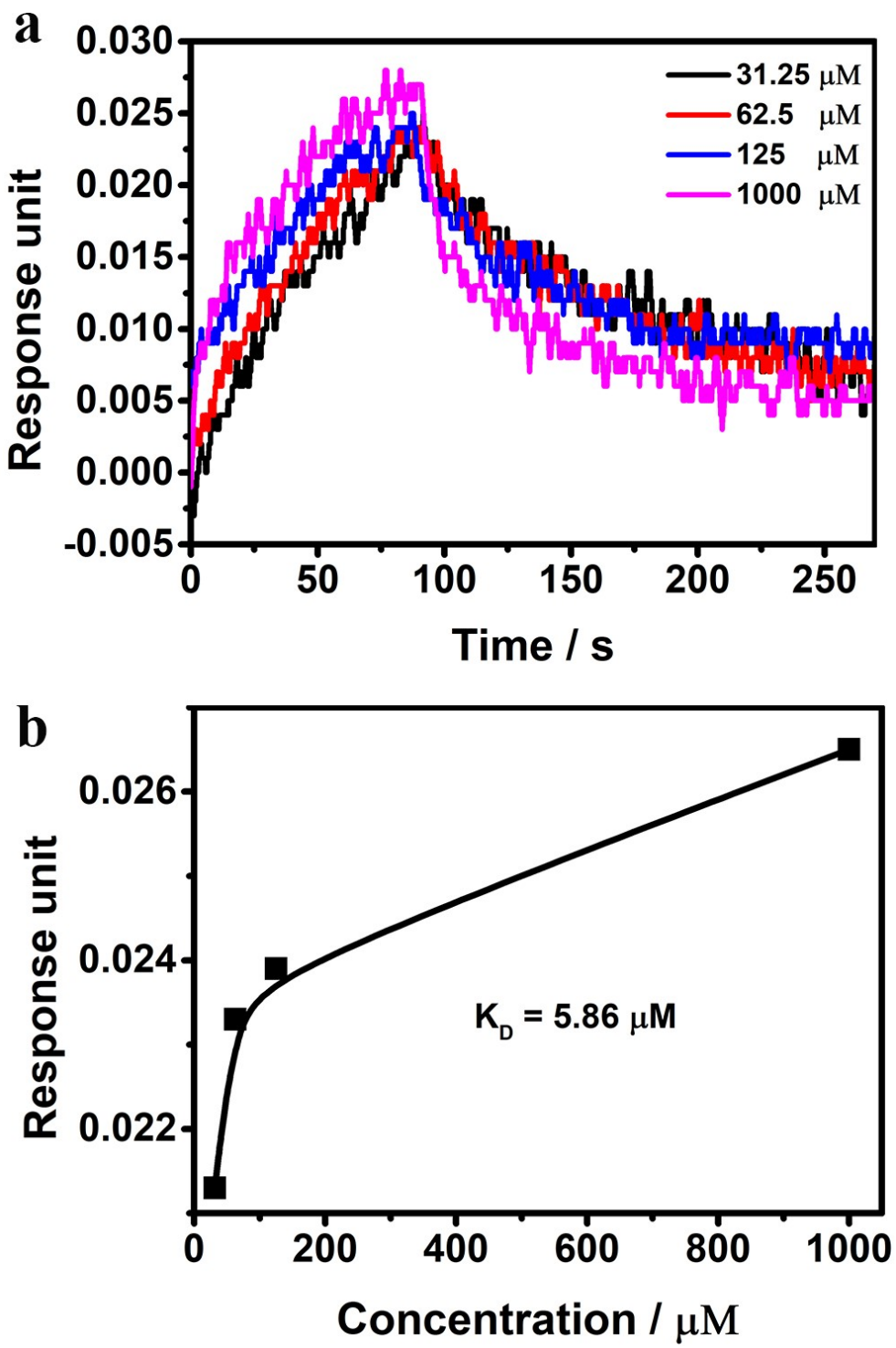

Figure S20. (a) Time dependency of BLI response curves of the CP-1 modified sensor in

response to different concentrations of DG12 solutions. (b) DG12 concentration-dependent response variation of the sensor.

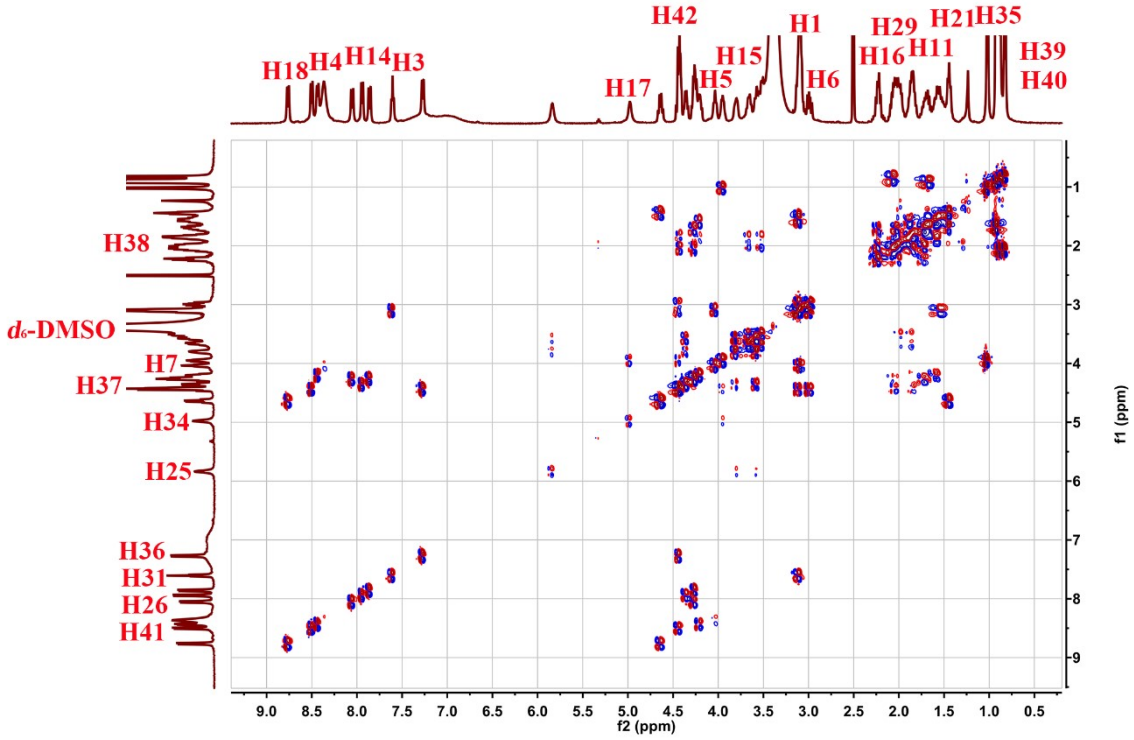

Figure S21. ^{1}H–^{1}H COSY spectrum of CP-1 (20 mM) in DMSO-d_6 at 25°C.

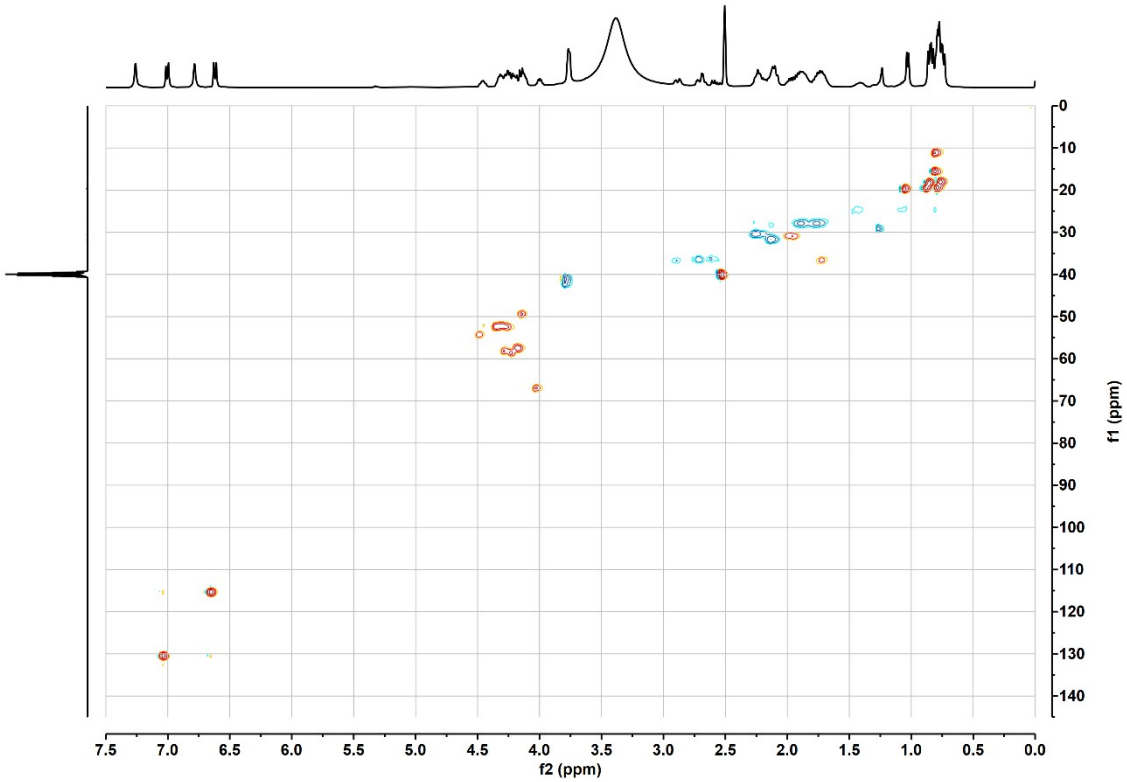

Figure S22. ^{13}C–^{1}H HSQC spectrum of CP-1 (20 mM) in DMSO-d_6 at 25°C. In the region above 7.5 ppm, there is no ^{13}C–^{1}H related peak, so it is not shown.

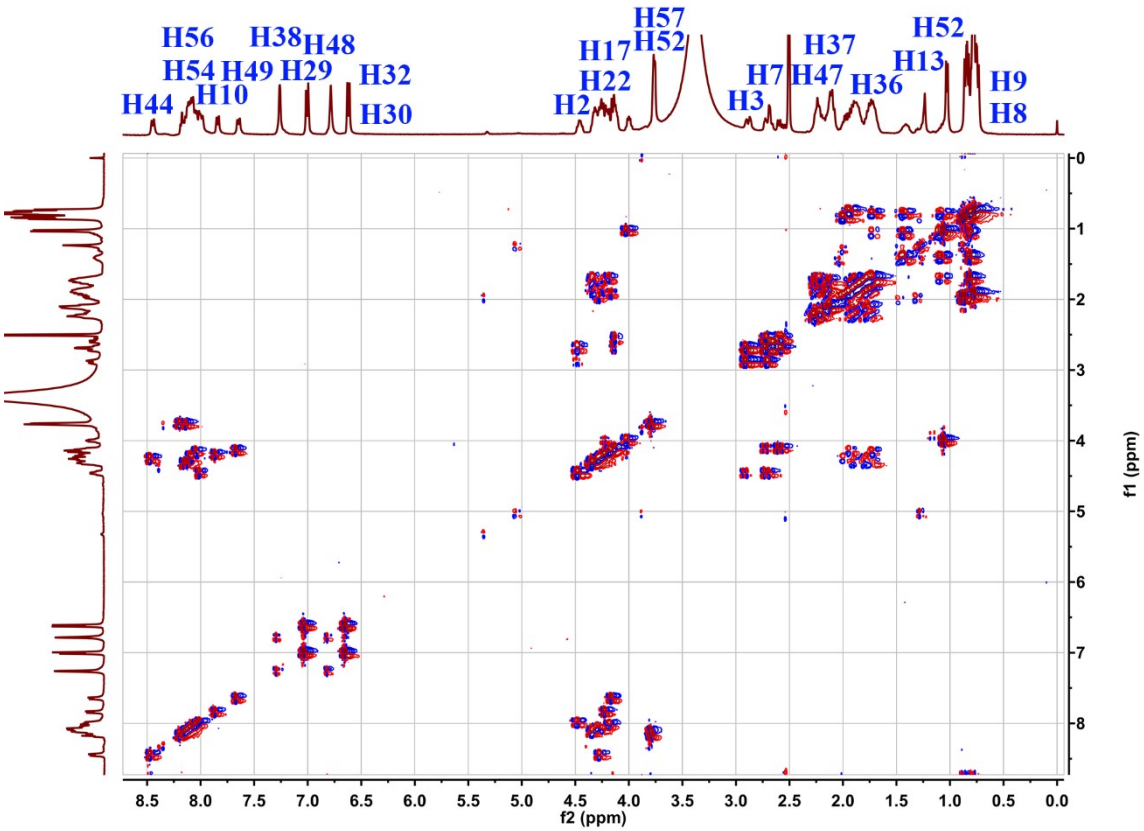

Figure S23. ^{1}H–^{1}H COSY spectrum of DG12 (20 mM) in DMSO-d_6 at 25°C.

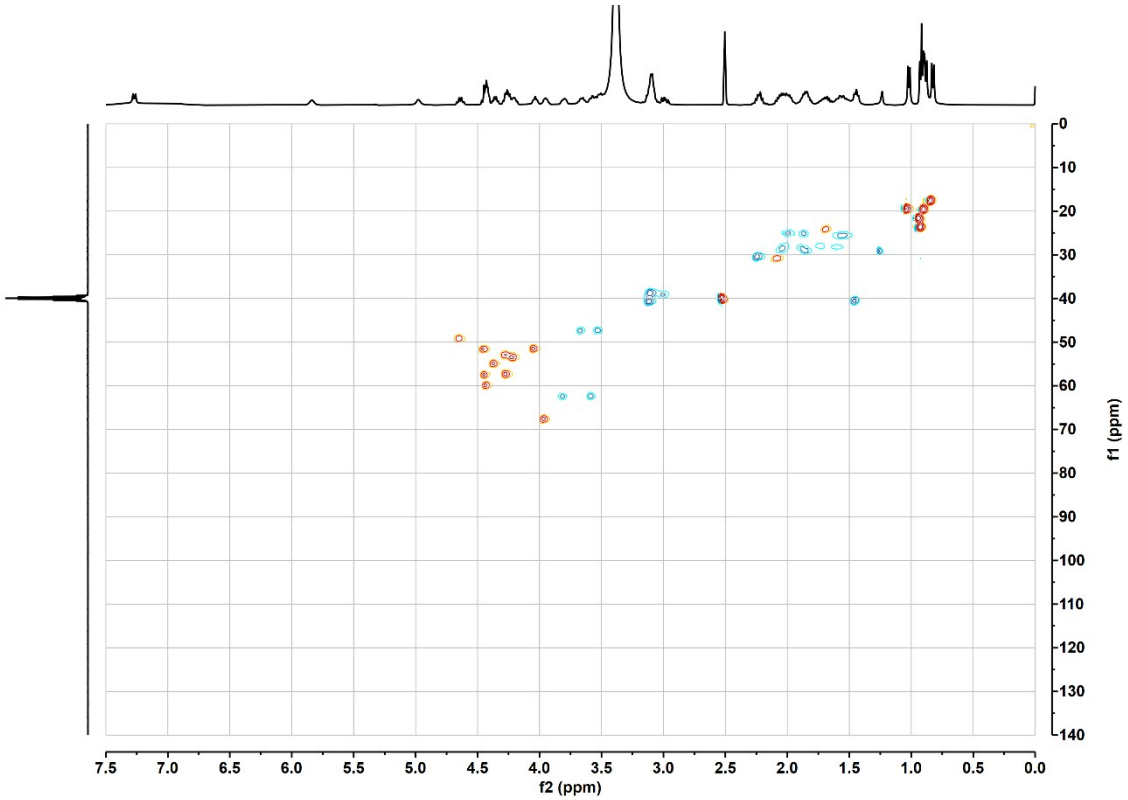

Figure S24. ^{13}C–^{1}H HSQC spectrum of DG12 (20 mM) in DMSO-d_6 at 25°C. In the region above 7.5 ppm, there is no ^{13}C–^{1}H related peak, so it is not shown.

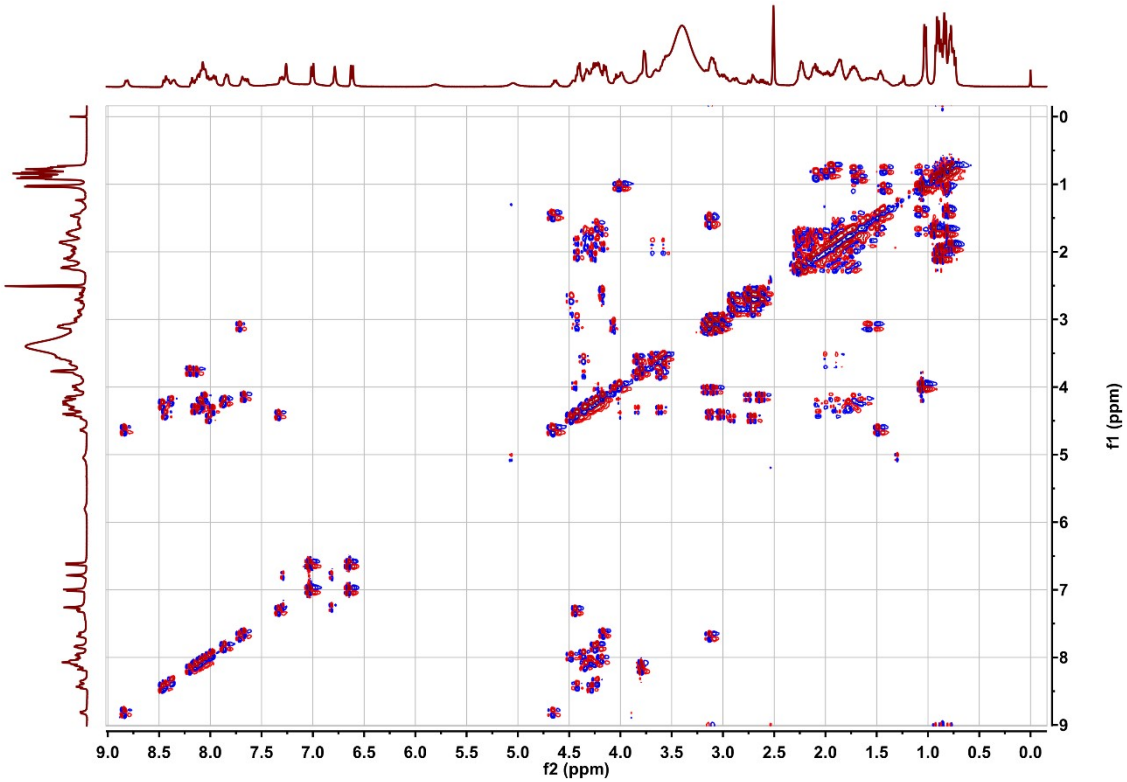

Figure S25. ^{1}H–^{1}H COSY spectrum of CP-1 with DG12 mixed at a molar ratio of 1:1 in DMSO-d_6 at 25°C.

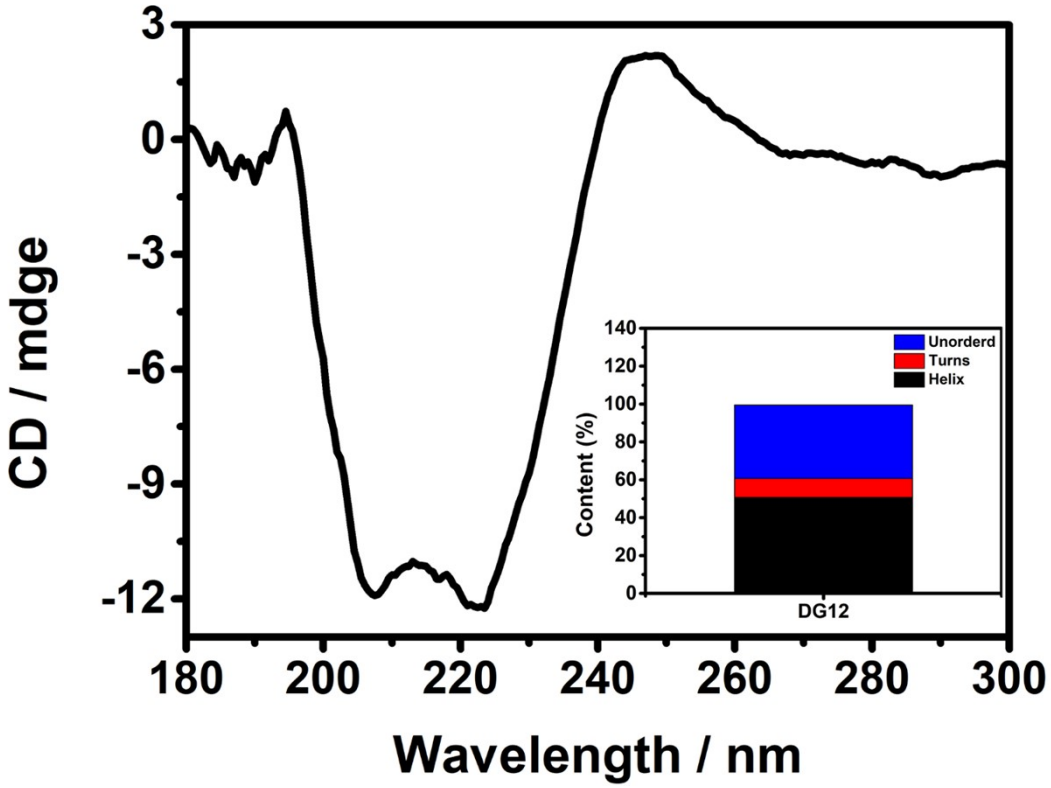

Figure S26. Circular dichroism (CD) spectrum of DG12 (1 mM).

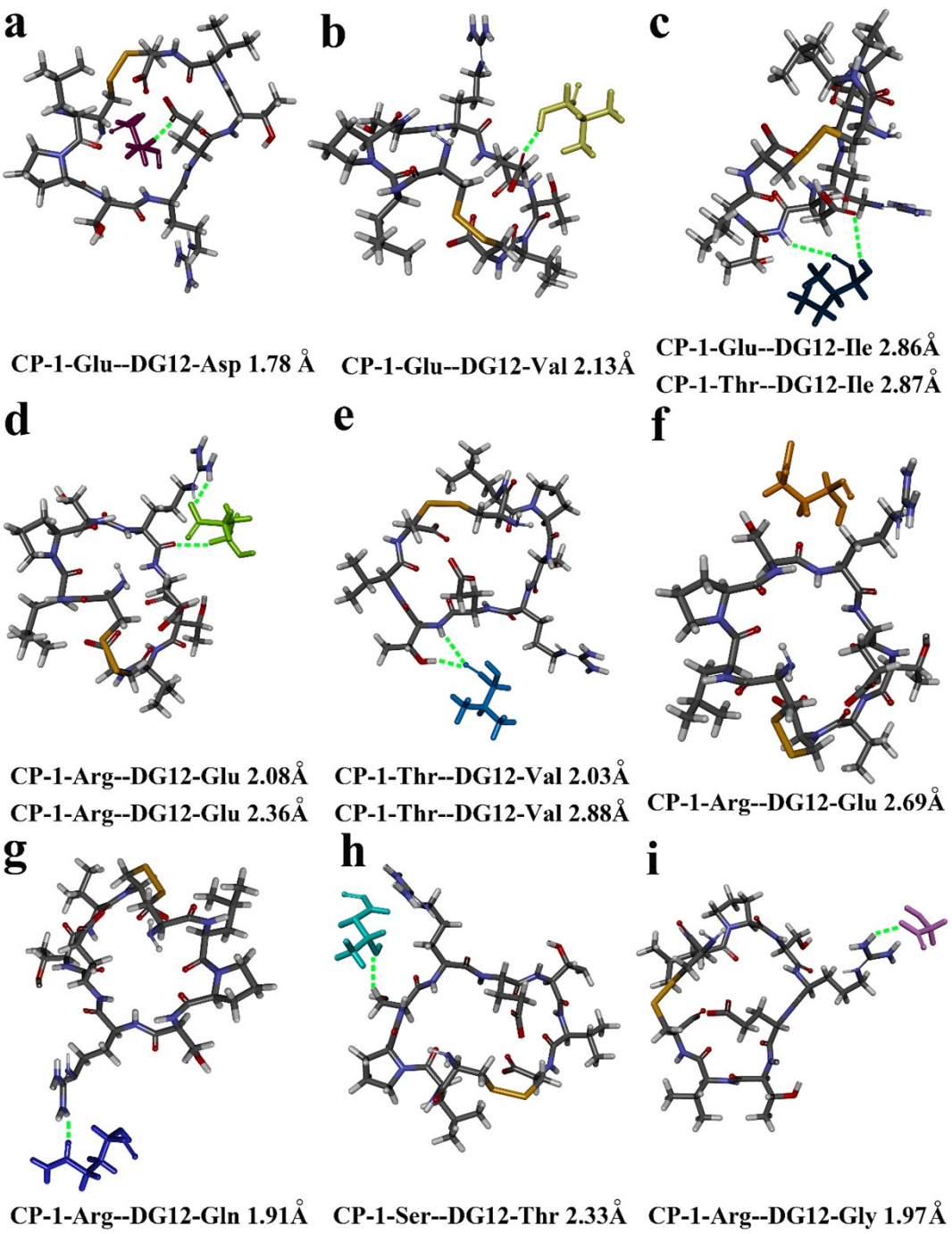

Figure S27. Molecular docking details of CP-1 and DG12, with hydrogen bonds shown as green dotted lines showing interactions between the species and adjacent amino acid residues. CP-1 full display, DG12 is shown alone with bound amino acids.

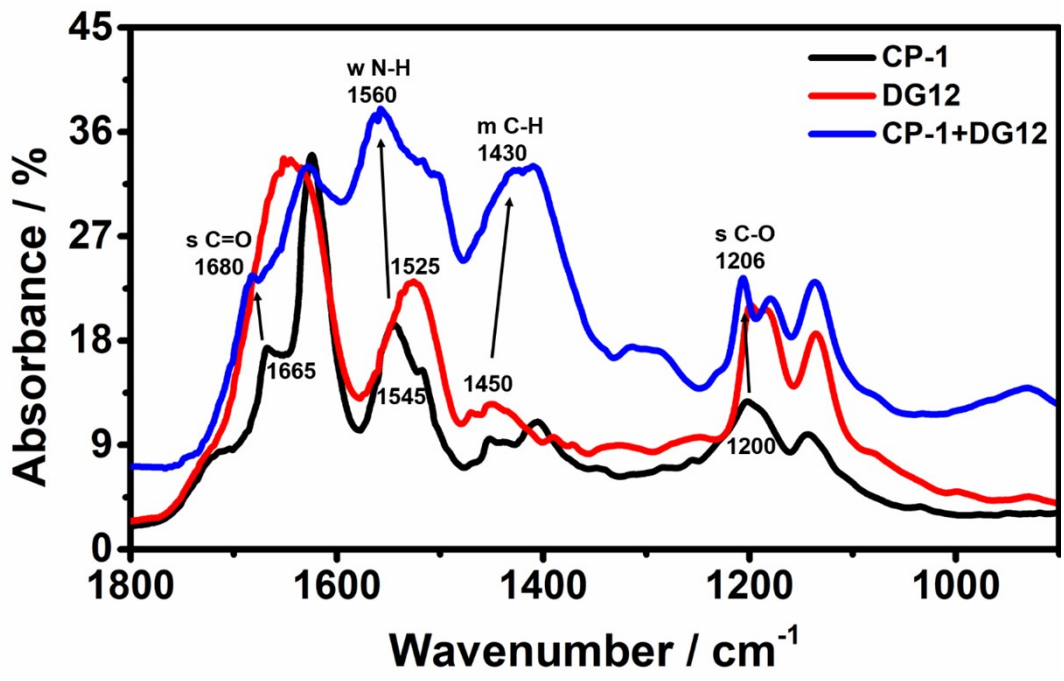

Figure S28. Selected IR spectra of 1 mM CP-1 (black), 1 mM DG12 (red) and their mixtures (blue), the mixture peaks show a clear variation, which indicates the presence of binding interactions between them.

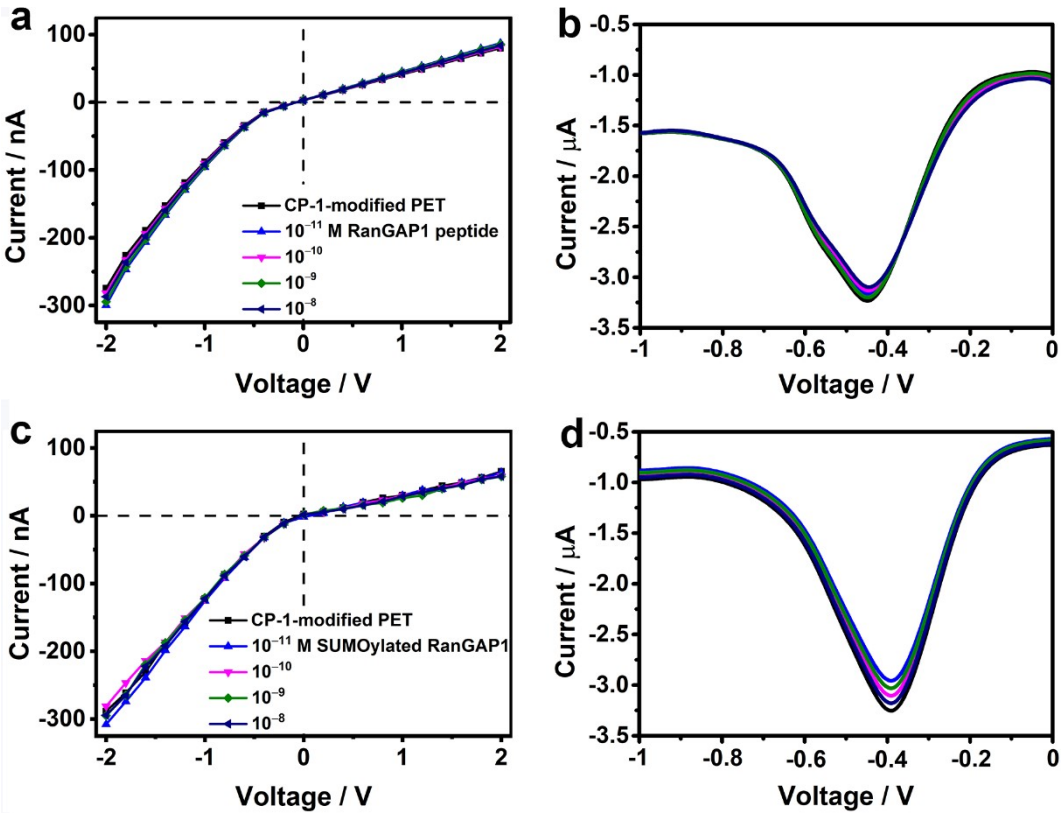

Figure S29. Transmembrane ionic current (a, c) and Faraday current (b, d) of CP-1-modified (a, b, c, d) in response to different concentrations of RanGAP1 (a, b) or SUMOylated RanGAP1 (c, d) in TBS (50 mM, pH 8.0) at 25°C.

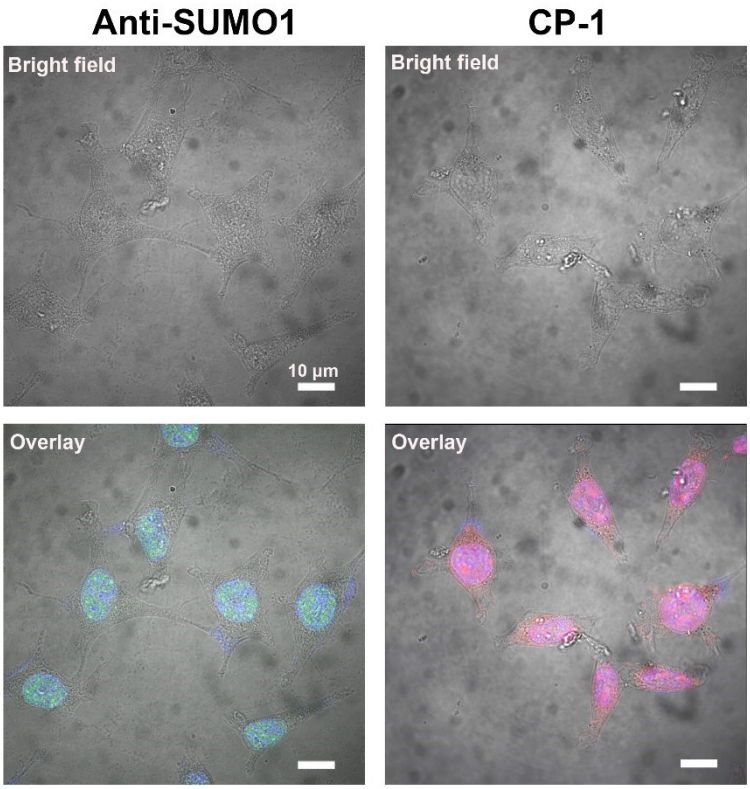

Figure S30. Imaging of SUMO1 with CP-1 in SH-SY5Y cells. Anti-SUMO1 antibody was used as a positive control (left panels). Rhodamine B-labelled CP-1 was used for immunofluorescence imaging (right panels). Scale bars: 10 µm.

References

1. Zhang, X.; Zhang, X.; Zhong, M.; Zhao, P.; Guo, C.; Li, Y.; Wang, T.; Gao, H., *ACS Chem. Neurosci.* **2020,** *11* (24), 4240-4253.
2. Zhang, X.; Zhong, M.; Zhao, P.; Zhang, X.; Li, Y.; Wang, X.; Sun, J.; Lan, W.; Sun, H.; Wang, Z.; Gao, H., *Biomater. Sci.* **2019,** *7* (12), 5197-5210.
3. Li, M.; Xiong, Y.; Wang, D.; Liu, Y.; Na, B.; Qin, H.; Liu, J.; Liang, X.; Qing, G., *Chem. Sci.* **2019,** *11* (3), 748-756.
4. P. Y. Apel; Y. E. Korchev; Z. Siwy; Spohr, R.; Yoshida, M., *Nucl. Instrum. Methods Phys. Res., Sect. B* **2001,** *184*, 337-346.
5. Scopece, P.; Baker, L. A.; Ugo, P.; Martin, C. R., *Nanotechnology* **2006,** *17* (15), 3951-3956.
6. Zhang, Z.; Li, P.; Kong, X. Y.; Xie, G.; Qian, Y.; Wang, Z.; Tian, Y.; Wen, L.; Jiang, L., *J. Am. Chem. Soc.* **2018,** *140* (3), 1083-1090.
7. Bhardwaj, A.; Kaur, J.; Wuest, M.; Wuest, F., *Nat. Commun.* **2017,** *8* (1), 461.
8. Ding, S.; Cao, S.; Zhu, A.; Shi, G., *Anal. Chem.* **2016,** *88* (24), 12219-12226.
9. Liu, G.; Zhang, G., *Springer Science & Business Media* **2013,** *pp*, 12-15.
10. John E. Ladbury; Klebe, G.; Freire, E., *Nat. Rev. Drug Discov.* **2010,** *9*, 23-27.
11. Klebe, G., *Nat. Rev. Drug Discov.* **2015,** *14* (2), 95-110.
12. Bishop, G. W.; Lopez, M. M.; Ramiah Rajasekaran, P.; Wu, X.; Martin, C. R., *J. Phys. Chem. C* **2015,** *119* (29), 16633-16638.
13. Miller, S. A.; Young, V. Y.; Martin, C. R., *J. Am. Chem. Soc.* **2001,** *123* (49), 12335-12342.
14. Pu Jin; Hitomi Mukaibo; Lloyd P. Horne; Gregory W. Bishop; Martin, C. R., *J. Am. Chem. Soc.* **2010,** *132*, 2118-2119.
15. Wang, X.; Wang, C.; Chu, H.; Qin, H.; Wang, D.; Xu, F.; Ai, X.; Quan, C.; Li, G.; Qing, G., *Chem. Sci.* **2020,** *11* (28), 7369-7378.
16. Morris, G. M.; Huey, R.; Lindstrom, W.; Sanner, M. F.; Belew, R. K.; Goodsell, D. S.; Olson, A. J., *J. Comput. Chem.* **2009,** *30* (16), 2785-2791.
17. Li, M.; Xiong, Y.; Lu, W.; Wang, X.; Liu, Y.; Na, B.; Qin, H.; Tang, M.; Qin, H.; Ye, M.; Liang, X.; Qing, G., *J. Am. Chem. Soc.* **2020,** *142* (38), 16324-16333.
18. Li, Y.; Sun, M.; Hu, Y.; Shan, Y.; Liang, Z.; Zhang, L.; Zhang, Y., *Anal. Chim. Acta* **2021,** *1154*, 338324.
19. Tokarz, P.; Woźniak, K., *Cancers* **2021,** *13* (9), 2059.